



Strathprints Institutional Repository

Yau, Wai-Lok and Pescher, Pascale and MacDonald, Andrea and Hem, Sonia and Zander, Dorothea and Retzlaff, Silke and Blisnick, Thierry and Rotureau, Brice and Rosenqvist, Heidi and Wiese, Martin and Bastin, Philippe and Clos, Joachim and Späth, Gerald (2014) The Leishmania donovani chaperone cyclophilin 40 is essential for intracellular infection independent of its stage-specific phosphorylation status. *Molecular Microbiology*, 93 (1). 80–97. ISSN 0950-382X , <http://dx.doi.org/10.1111/mmi.12639>

This version is available at <http://strathprints.strath.ac.uk/51396/>

Strathprints is designed to allow users to access the research output of the University of Strathclyde. Unless otherwise explicitly stated on the manuscript, Copyright © and Moral Rights for the papers on this site are retained by the individual authors and/or other copyright owners. Please check the manuscript for details of any other licences that may have been applied. You may not engage in further distribution of the material for any profitmaking activities or any commercial gain. You may freely distribute both the url (<http://strathprints.strath.ac.uk/>) and the content of this paper for research or private study, educational, or not-for-profit purposes without prior permission or charge.

Any correspondence concerning this service should be sent to Strathprints administrator: strathprints@strath.ac.uk

1 **The *Leishmania donovani* chaperone cyclophilin 40 is essential for intracellular infection**
2 **independent of its stage-specific phosphorylation status**

3 Wai-Lok Yau^{1,2}, Pascale Pescher¹, Andrea MacDonald², Sonia Hem³, Dorothea Zander², Silke
4 Retzlaff^{3,+}, Thierry Blisnick⁴, Brice Rotureau⁴, Heidi Rosenqvist^{5,++}, Martin Wiese⁵, Philippe
5 Bastin⁴, Joachim Clos², and Gerald F. Späth^{1,*}

6
7 Institut Pasteur and Centre National de la Recherche Scientifique URA 2581, ¹Unité de
8 Parasitologie Moléculaire et Signalisation, and ⁴Unité de Biologie Cellulaire des Trypanosomes,
9 25 rue du Dr Roux, F-75015 Paris, France; ²Clos Group (Leishmaniasis) and ³Electron
10 Microscopy Service, Bernhard-Nocht-Institut für Tropenmedizin, Bernhard-Nocht-Str. 74, D-
11 20359 Hamburg, Germany; ³Plate-forme de spectrométrie de masse protéomique - MSPP,
12 Biochimie et Physiologie Moléculaire des Plantes, UMR 5004 CNRS/UMR 0386
13 INRA/Montpellier SupArgo/Université Montpellier II, F-34060 Montpellier, France;
14 ⁵Strathclyde Institute of Pharmacy and Biomedical Sciences, University of Strathclyde,
15 Glasgow, Scotland, UK

16
17 * Correspondence: Gerald Späth

18 Institut Pasteur, 25 rue du Dr Roux, 75015 Paris, France

19 Phone: +33.1.40.61.38.58; Fax: +33.1.45.68.83.33

20 E-mail: gerald.spaeth@pasteur.fr

21 Short title: LdCyP40 null mutant analysis

22 Key words: *Leishmania donovani*, stress protein, cyclophilin 40, null mutant analysis,
23 intracellular survival, chaperone phosphorylation

24 +current address: Altona Diagnostics, Moerkenstr. 12, 22767 Hamburg, Germany

25 ++current address: Novo Nordisk, Novo Nordisk Park 1, DK-2760 Maaloev, Denmark

26 **Summary**

27 During its life cycle, the protozoan pathogen *Leishmania donovani* is exposed to contrasting
28 environments inside insect vector and vertebrate host, to which the parasite must adapt for
29 extra- and intracellular survival. Combining null mutant analysis with phosphorylation site-
30 specific mutagenesis and functional complementation we genetically tested the requirement of
31 the *Leishmania donovani* chaperone cyclophilin 40 (LdCyP40) for infection. Targeted
32 replacement of LdCyP40 had no effect on parasite viability, axenic amastigote differentiation,
33 and resistance to various forms of environmental stress in culture, suggesting important
34 functional redundancy to other parasite chaperones. However, ultra-structural analyses and
35 video microscopy of *cyp40*^{-/-} promastigotes uncovered important defects in cell shape,
36 organization of the subpellicular tubulin network and motility at stationary growth phase. More
37 importantly, *cyp40*^{-/-} parasites were unable to establish intracellular infection in murine
38 macrophages and were eliminated during the first 24h post infection. Surprisingly, *cyp40*^{-/-}
39 infectivity was restored in complemented parasites expressing a CyP40 mutant of the unique
40 S274 phosphorylation site. Together our data reveal non-redundant CyP40 functions in parasite
41 cytoskeletal remodeling relevant for the development of infectious parasites *in vitro*
42 independent of its phosphorylation status, and provides a framework for the genetic analysis of
43 *Leishmania*-specific phosphorylation sites and their role in regulating parasite protein function.

44

45

46 Introduction

47 Parasitic protozoa of the genus *Leishmania* are the etiological agents of leishmaniasis, severe
48 human diseases with clinical manifestations ranging from self-curing cutaneous lesions to fatal
49 visceral infection. During the infectious cycle, *Leishmania* replicate as extracellular flagellated
50 promastigotes in the midgut of female phlebotomine sand flies where they undergo an
51 environmentally triggered differentiation process termed metacyclogenesis to develop into
52 highly infectious metacyclic promastigotes (Sacks *et al.*, 1984). Following transmission by
53 blood feeding sand flies, metacyclic parasites are engulfed by phagocytes such as macrophages,
54 where they differentiate into non-motile amastigotes that cause the pathology of the disease.

55 *In vitro* differentiation of infectious metacyclic parasites is induced by nutritional
56 starvation or acidic pH, and development of amastigote-like cells in culture is triggered by pH
57 and temperature change (Zakai *et al.*, 1998; Cunningham *et al.*, 2001; Barak *et al.*, 2005),
58 suggesting that *Leishmania* stage-differentiation occurs through sensing of environmental stress
59 signals encountered inside insect and vertebrate hosts (Zilberstein *et al.*, 1994). Recently, a role
60 of stress signaling in parasite development has been suggested based on phosphoproteomics
61 studies. Gel-based proteomics approaches comparing enriched phosphoprotein fractions from
62 promastigotes and axenic amastigotes revealed a surprising divergence of the stage-specific
63 phosphoproteome with more than 30% of proteins showing statistically significant differential
64 phosphorylation (Morales *et al.*, 2008; Morales *et al.*, 2010). Phosphorylation events in
65 amastigotes were almost exclusively restricted to heat shock proteins and chaperones and
66 occurred largely at parasite-specific phosphorylation sites (Hem *et al.*, 2010), suggesting
67 regulation of the *Leishmania* response to stress by post-translational rather than classical
68 transcriptional mechanisms. This possibility has been investigated previously for the stress-
69 induced protein 1 (STI1), a chaperone that acts as a scaffolding protein for the assembly of
70 foldosome complexes (Pratt and Dittmar, 1998). Null mutant analysis of STI1 in *L. donovani*

71 established the requirement of this protein for parasite survival *in vitro*, and complementation
72 analysis by plasmid shuffle identified the two phosphorylation sites S15 and S481 as essential
73 for STI1 function and parasite viability (Morales *et al.*, 2010).

74 One group of stress proteins that showed increased phosphorylation in amastigotes in
75 these studies is represented by immunophilins, a protein family that includes cyclophilins
76 (CyPs) and FK506 binding proteins (FKBPs), which are characterized by a peptidyl-prolyl
77 isomerase activity required for proper protein folding (Barik, 2006). In a previous study, we
78 revealed stage-specific functions of cyclophilins using the CyP inhibitor cyclosporin A (CsA)
79 (Yau *et al.*, 2010). Inhibitor-treated promastigotes underwent non-synchronous cell cycle arrest
80 and acquired features similar to amastigotes, including oval shape and shortening of the flagella
81 reminiscent of *L. donovani* promastigotes treated with the HSP90 inhibitor Geldanamycin
82 (Wiesgigl and Clos, 2001). In contrast, treatment of axenic amastigotes resulted in parasite
83 death, a phenomenon that was abrogated by temperature shift from 37°C to 26°C. While this
84 pharmacological approach suggests potential roles of cyclophilins in parasite proliferation and
85 thermotolerance and sheds new light on the stage-specific action of CsA and its lethal effects
86 on intracellular *Leishmania* (Yau *et al.*, 2010), the pleiotropic inhibition of multiple
87 cyclophilins and the phosphatase calcineurin by CsA-CyP complexes (Chappell and Wastling,
88 1992) raise questions about the specific function of each of the 17 *Leishmania* cyclophilins.

89 The effects of CsA on *L. donovani* differentiation and thermotolerance, its binding to
90 parasite cyclophilin 40 (LdCyP40) (Yau *et al.*, 2010), and its stage-specific phosphorylation in
91 the axenic amastigotes prompted us to assess the role of this co-chaperone and its modification
92 in parasite survival and infectivity combining gene deletion, phosphoproteomics, and
93 complementation approaches. CyP40 is a highly conserved bi-functional protein that carries
94 peptidyl-prolyl isomerase (PPIase) activity and forms dynamic complexes in yeast and
95 mammalian cells with HSP90 through its conserved tetratricopeptide repeat (TPR) domains

96 (Hoffmann and Handschumacher, 1995). The loss-of-function study presented here identifies
97 important roles for LdCyP40 in the development of infectious parasites *in vitro* and
98 intracellular parasite survival independent of its phosphorylation status, thus establishing a
99 novel link between *L. donovani* chaperone activity and stress-induced parasite differentiation
100 relevant for host cell infection.

101

102 **Results**

103 *L. donovani* CyP40 is constitutively expressed but stage-specifically phosphorylated.

104 CyP40 belongs to the immunophilin superfamily that comprises 17 members in *Leishmania*
105 (Yau *et al.*, 2010). We first investigated the domain structure and sequence conservation of this
106 protein across trypanosomatid parasites (*L. major*, *L. infantum*, *L. braziliensis*, *T. brucei* and *T.*
107 *cruzi*) and various higher eukaryotes, including human, mouse, cow, and yeast. The putative
108 CyP40 protein sequences were retrieved from the UniProt (<http://www.uniprot.org/>) and
109 TriTrypDB databases (<http://tritrypdb.org/tritrypdb/>) by Blast search using *L. major* cyclophilin
110 40 (LmjF35.4770) as a query and aligned using ClustalW 2.0.12. *Leishmania* CyP40 displays
111 the characteristic two-domain structure (Fig. 1A). The N-terminal cyclophilin-like domain
112 (CLD) spans 171 residues and is highly conserved showing 68.8% of amino acid identity
113 across the analyzed organisms. This domain carries the enzymatic peptidyl-prolyl isomerase
114 (PPIase) function and is the target of the cyclophilin-specific inhibitor cyclosporin (CsA). The
115 functional residues for both PPIase activity and CsA binding are highly conserved as expected
116 from our previously published observations that *L. donovani* CyP40 carries isomerase activity
117 and can be enriched from crude parasite extracts by affinity chromatography using immobilized
118 CsA (Yau *et al.*, 2010). In addition, a cleft localized C-terminal of the CLD domain shows a
119 series of conserved residues that have been previously implicated in CyP40 chaperone activity
120 (Mok *et al.*, 2006). The C-terminal part of CyP40 contains three distinct TPR motifs that are

121 less conserved (50.4%, 47.3% and 50.2% of identity for TPR1, 2 and 3 respectively) and
122 together form the TPR domain known to interact with the conserved EEVD consensus
123 sequence of HSP70 and HSP90 (Ward *et al.*, 2002). Together these data identify *Leishmania*
124 CyP40 as a highly conserved member of the eukaryote immunophilin protein family that likely
125 interacts with HSPs and carries chaperone function.

126 In our previous proteomics studies on the protein phosphorylation dynamics during
127 *Leishmania* differentiation, *L. donovani* LdCyP40 abundance was significantly increased in the
128 phosphoproteome of axenic amastigotes when compared to promastigotes, suggesting
129 amastigote-specific phosphorylation of this protein (Morales *et al.*, 2008; Morales *et al.*, 2010).
130 However, this putative stage-specific phosphorylation has not been validated in *bona fide*
131 animal-derived amastigotes, and whether the increase of abundance results from an increase in
132 phospho-stoichiometry or simply increased protein expression has not been investigated. To
133 distinguish between these two possibilities, we analyzed LdCyP40 stage-specific expression
134 and phosphorylation profiles by Western blotting using total protein extracts and
135 phosphoprotein fractions enriched by immobilized metal affinity chromatography obtained
136 from cultured promastigotes, axenic amastigotes, and *bona fide* amastigotes purified from *L.*
137 *donovani* infected hamster spleen. As judged by α -tubulin expression used as normalization
138 control, LdCyP40 is constitutively expressed across all stages tested, but shows a significant
139 increase in abundance in the phosphoprotein fraction of axenic and hamster-derived
140 amastigotes (Fig. 1B) firmly establishing its stage-specific *de novo* phosphorylation and a
141 substantial increase in the phospho-stoichiometry of this protein.

142

143 *Establishment of cyp40^{-/-} null mutants.*

144 We established LdCyP40 null mutant parasites to study the biological functions of LdCyP40
145 and ultimately assess the physiological role of stage-specific CyP40 phosphorylation by

146 complementation. The endogenous alleles were replaced using two targeting constructs
147 comprising puromycin and bleomycin resistance genes flanked by the 5' and 3'UTRs of
148 LdCyP40 (Fig. 2A and Fig. S1). Respective add-back controls re-expressing LdCyP40 from the
149 ribosomal locus under the control of the CyP40 3'UTR were generated using a knock-in
150 strategy (Fig. 2A and Fig. S2). The absence of the LdCyP40 ORF and corresponding protein in
151 six independent null mutant clones and its re-expression in complemented parasites was
152 confirmed by PCR (Fig. 2B and data not shown) and Western blot analysis (Fig. 2C and Fig.
153 S3).

154

155 *Morphological characterization of cyp40^{-/-} null mutant and add-back clones.*

156 Microscopic observation of the two independent null mutant clones *cyp40^{-/-}* cl.4 and cl.5 and
157 four independent add-back clones as well as add-back pools derived from each null mutant
158 clone revealed important morphological alternations at stationary growth phase that correlated
159 with the absence of CyP40 expression (Fig. 3A and Fig. S4). At logarithmic growth phase,
160 CyP40 null mutant promastigotes were morphologically identical to wild-type and add-back
161 controls as judged by Giemsa staining of fixed parasite cultures (Fig. 3A, upper panels). By
162 contrast 70% of *cyp40^{-/-}* cells at stationary growth phase of two independent null mutant clones
163 acquired a small spherical cell shape, while wild-type parasites and add-back clones showed the
164 spindle shaped cell body characteristic for stationary phase parasites (Fig. 3A, lower panels,
165 and Fig. S4). Moreover, measurements of cell body and flagellum length revealed a significant
166 reduction of the ratio between both parameters in *cyp40^{-/-}* cells (Fig. S4B). Given the
167 reproducibility of this phenotype, most of the subsequent experiments were performed with
168 *cyp40* null mutant clone 4 and its corresponding add-back pool if not otherwise stated.

169 As cell rounding is often associated with cellular stress and apoptotic cell death (Lee *et*
170 *al.*, 2002; Gannavaram and Debrabant, 2012), we next investigated integrity and ultra-structural

171 organization of CyP40 null mutant cells and controls. Wild-type, *cyp40*^{-/-} and *cyp40*^{-/+}
172 promastigotes were fixed with 2% glutaraldehyde and analyzed by scanning electron
173 microscopy (Fig. 3B). This analysis confirmed the atypical spherical cell shape of *cyp40*^{-/-}
174 stationary phase promastigotes and provided a first indication of their cellular integrity.
175 Likewise, analysis by transmission electron microscopy revealed no overt alterations in cellular
176 organization of *cyp40*^{-/-} cells, which showed intact nuclei and mitochondria, and absence of
177 apoptotic bodies or autophagosomes (Fig. 3C). Finally, direct assessment of cell death by
178 FACS analysis following membrane exposure of phosphatidylserine with annexin V-FITC and
179 exclusion of propidium iodide did not reveal any significant change in cell viability of
180 stationary *cyp40*^{-/-} parasites after 6 days of *in vitro* culture (Fig. 3D). Together these results
181 rule out the possibility of cell death as the cause of *cyp40*^{-/-} morphological alterations but
182 rather suggest a defect in parasite development and cellular remodeling at stationary phase.

183

184 *Phenotypic characterization of stationary phase cyp40*^{-/-} promastigotes.

185 During the infectious cycle, non-infectious procyclic promastigotes differentiate into highly
186 infective metacyclic promastigotes in response to nutritional starvation after digestion and
187 excretion of the blood meal. This process is mimicked in culture during stationary growth
188 phase (Sacks *et al.*, 1984; da Silva and Sacks, 1987) and is accompanied by the expression of
189 characteristic biological and morphological markers, including expression of high molecular
190 weight LPG and increase in SHERP mRNA abundance. The altered morphology of *cyp40*^{-/-}
191 parasites primed us to investigate the status of these phenotypic markers. First, monitoring cell
192 density of WT, *cyp40*^{-/-} and add-back promastigotes with a CASY cell counter, deletion of
193 CyP40 did not affect the rate of proliferation nor the density reached at stationary phase (Fig.
194 4A). Surprisingly, despite defects in stationary phase morphology, *cyp40*^{-/-} promastigotes
195 showed normal expression of higher molecular weight LPG characteristic for stationary phase

196 parasites as revealed by Western blot analysis using the anti-LPG antibody CA7AE (Fig. 4B),
197 and induced SHERP mRNA to levels corresponding to WT and add-back controls (Fig. 4C).
198 Together these data demonstrate that *L. donovani* CyP40 is dispensable for parasite survival *in*
199 *vitro* under standard culture conditions, and is not required for metacyclic-specific glycolipid
200 remodeling or gene regulation, at least for the markers investigated here. To further
201 characterize the stationary phase defect of *cyp40*^{-/-} parasites, we investigated the functional
202 properties of infectious, stationary phase parasites, including cell motility and intracellular
203 survival.

204
205 *CyP40 null mutants show reduced motility and a loosened sub-pellicular tubulin network.*

206 An important functional characteristic of stationary phase parasites is a significant increase in
207 motility, which is of physiological relevance in the natural setting for migration of metacyclic
208 parasites from sand fly midgut to larynx (Walters *et al.*, 1989; Walters *et al.*, 1993), or the
209 establishment of host cell infection (Uezato *et al.*, 2005; Forestier *et al.*, 2011). We quantified
210 motility in at least 741 WT, *cyp40*^{-/-} and add-back promastigotes obtained from logarithmic
211 and stationary phase cultures utilizing video microscopy and *in silico* tracking analysis.
212 Qualitative observation of each movie did not reveal any significant difference in flagellar
213 wave orientation and flagellar beating amplitude across all lines and both culture conditions
214 (data not shown). Likewise, quantitative analysis showed no significant difference in beating
215 frequencies and speed between WT, *cyp40*^{-/-}, and add-back log phase promastigotes. As
216 expected, WT and add-back promastigotes showed a statistically significant increase in motility
217 speed and flagellar beat frequency at stationary phase (Fig. 5A), and moved in a uni-directional
218 way over extended distances (Fig. 5B and Video S1). By contrast, CyP40 null mutant parasites
219 do not increase speed at stationary growth phase (Fig. 5A) and show a defect in directional
220 motility as they largely spin on themselves (Fig. 5B and Video S1).

221 As judged by transmission electron microscopy, this motility defect was not caused by
222 alterations in flagellar structure of *cyp40*^{-/-} parasites, which maintained the characteristic 9+2
223 organization of the axoneme (Fig. 5C). However, investigating more closely the *Leishmania*
224 sub-pellicular tubulin network by scanning EM after removal of the parasite plasma membrane
225 by detergent treatment, stationary phase *cyp40*^{-/-} promastigotes showed a significantly
226 loosened tubulin network, in contrast to the very dense, small-meshed network observed in
227 wild-type parasites (Fig. 5D). Western blot analysis of WT, *cyp40*^{-/-} and add-back parasites
228 from log and stationary cultures did not reveal any significant difference in expression levels of
229 α - and β -tubulin, with the exception of a small β -tubulin isoform at around 33kDa, which is
230 specific for stationary phase cells and slightly reduced in CYP40 null mutants (Fig. 5E). These
231 data demonstrate non-redundant CYP40 functions in cytoskeletal remodeling of the parasite
232 during stationary growth phase, which is likely the basis for the aberrant morphology and the
233 motility defect observed in *cyp40*^{-/-} parasites.

234

235 *Leishmania cyp40*^{-/-} mutants fail to establish intracellular infection.

236 The development of highly infectious metacyclic parasites can be mimicked by exposing
237 promastigotes to various forms of stress, including nutritional starvation and acidification at
238 stationary phase (da Silva and Sacks, 1987; Bate and Tetley, 1993; Zakai *et al.*, 1998; Serafim
239 *et al.*, 2012). The stationary phase-specific defects of *cyp40*^{-/-} promastigotes primed us to
240 investigate their capacity to infect host cells. Bone marrow-derived macrophages obtained from
241 C57BL/6 mice were incubated for 2 hours with WT, *cyp40*^{-/-}, and add-back stationary phase
242 promastigotes at a multiplicity of infection of 10 parasites per host cell, free parasites were
243 removed by washing, and intracellular parasite burden was determined by nuclear staining and
244 fluorescence microscopy at 2, 24, and 48 hours post infection. The *cyp40*^{-/-} cells were
245 phagocytosed at levels comparable to the controls with 80% of macrophages hosting a mean of

246 2.5 parasites per infected host cell (Fig. 6A). While WT and add-back parasites persisted over
247 the 48 hours post infection period and showed intracellular proliferation as documented by the
248 increase in number of parasites per infected macrophage (Fig. 6A, lower panel), the level of
249 *cyp40*^{-/-} infection was reduced by over 90% during the first 24 hours and parasites were
250 completely eliminated by 48 hours post infection (Fig. 6A). We next tested if intracellular
251 elimination of *cyp40*^{-/-} parasites is caused by a susceptibility to elevated temperature or acidic
252 pH encountered inside the host cell, or results from a defect in amastigote differentiation.
253 CyP40 null mutant promastigotes grown at 37°C did not show any significant difference to WT
254 and add-back parasites (Fig. S7A), and axenic amastigotes developed and proliferated normally
255 in response to both temperature and pH shift as judged by cell counting (Fig. 6B) and
256 assessment of expression of the axenic amastigote marker protein A2 (Fig. 6C). Thus,
257 LdCyP40 carries essential functions for successful host cell infection independent of parasite
258 resistance to acidic pH, elevated temperature, or amastigote development.

259

260 *Functional assessment of CyP40 phosphorylation.*

261 The failure of *cyp40*^{-/-} parasites to establish intracellular infection provided an interesting read
262 out to test for the function of CyP40 phosphorylation in parasite infectivity using
263 complementation analysis. We investigated the CyP40 amino acid residues that were
264 phosphorylated by using LC-ESI-MS/MS analysis. Axenic amastigote protein extracts from
265 transgenic *L. donovani* over-expressing Strep::*CyP40* were collected and Strep::*CyP40* was
266 enriched by affinity chromatography using streptactin agarose liquid chromatography (Fig. S5).
267 After SDS-PAGE and Coomassie Brilliant Blue staining, the band corresponding to
268 Strep::*CyP40* was extracted and subjected to phosphopeptide analysis by LC-ESI-MS/MS. MS
269 analysis revealed that residue serine 274 (S274) of *CyP40* was the only detected
270 phosphorylation site of *CyP40* in axenic amastigotes (Fig. 7A and Fig. S8). The multiple

271 sequence alignment of trypanosomatid CyP40 described in Fig. 1 localizes S274 to the center
272 of the TPR motif 2 and shows that it is unique among trypanosomatids (Fig. 7B). An
273 independent study also pointed out that S274 is phosphorylated in *L. mexicana* (Dr. Martin
274 Wiese, University of Strathclyde, Glasgow, unpublished data). These data suggest that
275 phosphorylation at S274 of CyP40 is *Leishmania*-specific and may have critical roles in
276 parasite survival.

277 To study the relationship between CyP40 phosphorylation and parasite infectivity, an
278 add-back line was generated expressing a serine 274 to alanine (S274A) phosphorylation site
279 mutant version of CyP40 (Fig. 7C, left panel, and Fig. S6), which was subsequently tested for
280 *in vitro* infectivity. We next assessed the accumulation of this mutant in the parasite phospho-
281 protein fraction to test if elimination of S274 is sufficient to abrogate phospho-specific affinity
282 purification of CyP40. Total protein extracts and phospho-protein enriched extracts from WT
283 treated or not with lambda phosphatase, or add-back parasites expressing CyP40-S274A were
284 analyzed by western blotting using anti-CyP40 antibody and anti- α -tubulin antibody for
285 normalization of the signals. As expected, robust amounts of CyP40 were detected in the wild-
286 type phospho-protein extracts, and this signal was strongly reduced by phosphatase treatment
287 prior to enrichment representing background levels of CyP40 enrichment likely due to non-
288 specific binding to the affinity matrix (Fig. 7C, right panel). The same level of background
289 signal was obtained with CyP40-S274A confirming that this residue represents the only
290 phosphorylation site in CyP40.

291 Bone marrow-derived macrophages were then infected with *cyp40*^{-/-} promastigotes
292 complemented with CyP40-S274A. The controls, WT, *cyp40*^{-/-} and add-back promastigotes
293 behaved in a similar fashion as described previously (Fig. 7D). The higher counts of infected
294 macrophage obtained with WT parasites compared to add-back control may be due to batch-to-
295 batch variation of parasites. The *cyp40*^{-/-}+S274A add-back promastigotes entered

296 macrophages and established infection at similar efficiency. The parasite number decreased in
297 the first 24 hours post infection but parasites started to multiply after 48 hours (Fig. 7D, left
298 panel). The intracellular proliferation of CyP40-WT and CyP40-S274A add-back did not show
299 any significant difference, as indicated by the number of parasites per 100 macrophages at 48
300 hours post infection (Fig. 7D, right panel). These data indicate that phosphorylation of CyP40
301 is either not important for the function of CyP40 in *Leishmania* intracellular survival, or can be
302 compensated by other co-chaperones.

303

304

305 Discussion

306 The conserved co-chaperone CyP40 participates in the formation of highly dynamic heat shock
307 protein complexes across various eukaryotes (Pratt *et al.*, 2004; Ratajczak *et al.*, 2003; Riggs *et*
308 *al.*, 2004; Pearl and Prodromou, 2006), and has been linked to many tissue- and organism-
309 specific functions, including steroid receptor signaling in mammalian cells and yeast (Ratajczak
310 *et al.*, 2009), or microRNA activity and assembly of RNA-induced silencing complexes (RISCs)
311 in plants (Smith *et al.*, 2009; Ilki *et al.*, 2012). No information is available on how this co-
312 chaperone affects viability and infectivity of trypanosomatid pathogens, including *Leishmania*,
313 even though parasite differentiation is triggered by environmental stress signals (Zilberstein
314 and Shapira, 1994), has been previously linked to the formation of heat shock complexes
315 (Morales *et al.*, 2010), and is regulated by HSP90 activity (Wiesgigl and Clos, 2001). Here by
316 utilizing a targeted null mutant approach we reveal non-redundant and essential CyP40
317 functions in *Leishmania* stage-specific morphogenesis, motility, and the development of
318 infectious-stage parasites.

319 The superfamily of immunophilin proteins is divided into cyclophilins (CyPs) and FK-
320 binding proteins (FKBPs) based on their interaction with the immunosuppressive drugs CsA
321 and FK506, respectively (McCaffrey *et al.*, 1993; Ho *et al.*, 1996). All immunophilins share a
322 highly conserved peptidyl-prolyl isomerase (PPIase) domain implicated in proper folding of
323 nascent proteins (Galat, 2003). Three members of this protein family have attracted
324 considerable interest due to their interaction with HSP90 and their implication in heat shock
325 complex formation, CyP40, FKBP51 and FKBP52. Despite considerable differences in their
326 sequence and structure, these proteins are functionally related through their PPIase enzymatic
327 activity and the presence of a conserved C-terminal TPR domain that confers interaction with
328 HSP90. By dynamically competing for HSP90 binding, both CyP40 and FKBP52 co-
329 chaperones have been shown to establish distinct steroid hormone receptor complexes in

330 mammals and yeast (Pratt and Toft, 1997; Ratajczak et al., 2003; Riggs et al., 2004). The
331 absence of steroid hormone receptor signaling in *Leishmania* and related trypanosomatids
332 raises the question on the parasite-specific functions of CyP40.

333 We recently obtained first insight into the biological roles and functional diversity of *L.*
334 *donovani* CyPs and FKBP s using a pharmacological approach. Treatment of *L. donovani*
335 promastigotes and axenic amastigotes with CsA and FK506 revealed important, redundant
336 functions of CyPs and FKBP s in promastigote proliferation and morphogenesis, but unique
337 function of *Leishmania* CyPs in parasite thermotolerance (Yau *et al.*, 2010). The direct
338 enrichment of CyP40 from *L. donovani* extracts using immobilized CsA, the presence of a
339 conserved TPR domain in this protein, and its stage-specific phosphorylation in axenic
340 amastigotes (Morales *et al.*, 2008; Morales *et al.*, 2010) suggested important stress functions of
341 CyP40 in *Leishmania* differentiation and thermotolerance that may be regulated at post-
342 translational levels.

343 However, the CyP40 loss of function analysis performed in this study shed a
344 substantially different light on the protein's unique functions. In contrast to CsA treated
345 promastigotes that underwent non-synchronous cell cycle arrest at logarithmic growth phase
346 and showed morphological changes reminiscent of axenic amastigotes, i.e. retraction of the
347 flagellum and oval cell body (Yau *et al.*, 2010), *cyp40*^{-/-} promastigotes did not show any overt
348 defects in cell growth or cell shape at this culture stage. Moreover, absence of CyP40
349 expression did neither alter the IC50 to CsA nor did it affect the phenotypic response to this
350 inhibitor (Fig S7 and data not shown) suggesting that CyP40 is not a major target of CsA at this
351 culture stage. Finally, *cyp40*^{-/-} parasites did not show any overt defects in resistance to various
352 forms of stress, including nutritional starvation, acidic pH and elevated temperatures (Fig. 6D
353 and S7), while CsA-treated parasites underwent cell death at 37°C (Yau *et al.*, 2010). Thus, in
354 contrast to other TPR domain containing chaperones in *Leishmania*, such as STI1 (Morales *et*

355 *al.*, 2010; Hombach *et al.*, 2013) or SGT (Ommen *et al.*, 2010), which are both essential for
356 *Leishmania* promastigote viability, CyP40 carries non-essential functions at this stage, which
357 may be redundant to other PPIases of the CyP or FKBP protein families and thus compensated
358 in the null mutant.

359 Various aspects of the *cyp40*^{-/-} null mutant phenotype pointed at essential and non-
360 redundant CyP40 functions that were not observed during CsA treatment and thus are likely
361 independent of the CyP40 PPIase activity targeted by this inhibitor (Yau *et al.*, 2010). First,
362 lack of CyP40 expression caused important morphological and structural alterations of
363 stationary phase parasites, which adopted a rounded rather than characteristic needle-shaped
364 morphology. These defects were linked to a loosening of the sub-pellicular tubulin network that
365 determines parasite morphology and provides the rigidity necessary for efficient motility
366 (Seebeck *et al.*, 1990). These results point to unique CyP40 functions in regulating *Leishmania*
367 cytoskeletal dynamics. Microtubule elongation and shortening are highly dynamic events that
368 are regulated by stabilizing or destabilizing interactions (Walczak, 2000). Recently, a role of
369 the CyP40 related immunophilin FKBP52 in regulating microtubule depolymerization through
370 direct interaction with tubulin via its TPR domain has been described in rat brain (Chambraud
371 *et al.*, 2007). Given the capacity of CyP40 and FKBP52 to compete for molecular partners
372 (Ratajczak *et al.*, 2003), it is possible that CyP40 interacts with microtubules and promotes
373 tubulin polymerization to counteract FKBP52-mediated depolymerization. Alternatively, the
374 requirement of CyP40 for *Leishmania* morphological integrity at stationary growth phase may
375 be indirect and caused by misfolding of client proteins that require CyP40 co-chaperone
376 function. In yeast, TPR-domain containing co-chaperones make distinct and extensive contacts
377 with HSP90 that lead to a differential modulation of HSP90 chaperone function (Ratajczak *et al.*,
378 2009). For example, displacement of STI1 from HSP90 by the yeast CyP40 homolog CPR6
379 restores ATPase activity (Pearl and Prodromou, 2006). Based on our previous observation that

380 *L. donovani* STI1 acts as a scaffolding protein to assemble highly dynamic heat shock
381 complexes (Morales *et al.*, 2010), it is possible that lack of CyP40 alters the formation and
382 activity of foldosome complexes causing the observed phenotypic consequences of CyP40
383 deletion.

384 Second, *cyp40*^{-/-} parasites showed an important, stage-specific defect in directional
385 motility despite integrity of the 9+2 structure of the axoneme. The presence of trypanosomatid
386 CyP40 in the flagellar proteome (Oberholzer *et al.*, 2011) indicates that LdCyP40 may directly
387 interact with motor components for proper folding. This possibility is supported by various
388 studies of related FKBP52 PPIase domain and the motor protein dynein via dynamitin (Silverstein *et al.*, 1999; Galigniana *et al.*, 2001;
389 Galigniana *et al.*, 2004), (ii) an essential role of FKBP52 for sperm tail development and
390 movement (Hong *et al.*, 2007), and (iii) a requirement of FKBP12 in *Trypanosoma brucei*
391 motility (Brasseur *et al.*, 2013).

393 Finally, the most striking loss-of-function phenotype of *cyp40*^{-/-} parasites is represented
394 by the abrogation of intracellular parasite survival. While we cannot rule out that loss of
395 intracellular survival reflects a developmental defect caused by the morphological and
396 cytoskeletal alterations observed at stationary phase culture, our observations that null mutant
397 parasites are normal in viability and metacyclic marker expression, and convert normally into
398 axenic amastigotes may point to different possible scenarios. Intracellular killing of *cyp40*^{-/-}
399 mutants may be associated with the requirement of LdCyP40 co-chaperone activity for proper
400 folding of parasite survival factors, which may confer parasite resistance to macrophage
401 cytolytic activities. Alternatively, the identification of LdCyP40 in the parasite secretome
402 (Silverman *et al.*, 2008) opens the possibility that this co-chaperone may directly interact with
403 host phagolysosomal or cytoplasmic proteins to subvert host cytolytic activities and favor
404 intracellular parasite survival, a scenario reminiscent to secreted *T. cruzi* CyP19, which

405 inactivates the anti-microbial peptide trialysin of the reduviid insect vector by direct binding
406 (Kulkarni *et al.*, 2013). A third possibility is the involvement of CyP40 in the sorting of
407 exosome payload proteins, similar to the role played by the chaperone HSP100 (Silverman *et*
408 *al.*, 2010). This idea would be supported by the very similar phenotypes of CyP40 (this paper)
409 and HSP100 null mutants (Krobitsch and Clos, 1999).

410 In previous phosphoproteomics investigations we identified LdCyP40 as a major
411 amastigote-specific phosphoprotein and revealed a coordinated increase in phosphorylation of
412 all major parasite chaperones and HSPs during axenic amastigote differentiation, which
413 occurred largely at parasite-specific sites (Morales *et al.*, 2008; Morales *et al.*, 2010; Hem *et al.*,
414 2010). These results are compatible with the hypothesis that *Leishmania* stress protein function
415 is regulated at post-translational levels through phosphorylation by stress-activated protein
416 kinases, a possibility that is supported by the genetic validation of two phosphorylation sites in
417 *L. donovani* STI1 that are essential for parasite viability (Morales *et al.*, 2010). The failure of
418 *cyp40*^{-/-} parasites to establish intracellular infection provided a powerful read out to further test
419 this hypothesis and to assess the physiological role of CyP40 phosphorylation by site-directed
420 mutagenesis of the single CyP40 phosphorylation site. Surprisingly, although CyP40
421 phosphorylation at S274 was highly stage-specific and observed exclusively in axenic and *bona*
422 *fide* splenic amastigotes, expression of an LdCyP40 S274A mutant fully restored intracellular
423 survival of *cyp40*^{-/-} parasites thus ruling out an essential role of this modification in
424 intracellular infection *in vitro*. The biological function of this highly conserved phosphorylation
425 site eludes us. Phosphorylation of FKBP52 disrupts the binding activity of this chaperone to
426 HSP90 and thus is required for the dynamic turnover of heat shock complexes (Miyata *et al.*,
427 1997). The S274 CyP40 phosphorylation site maps to the TPR2 sub-domain and thus may play
428 a similar role in regulating the dynamics of protein-protein interactions, but may not cause a

429 discernible phenotype due to the expression of other, functionally redundant TPR-domain
430 proteins in *Leishmania*.

431 In conclusion, null mutant analysis of LdCyP40 revealed important non-redundant
432 functions of this co-chaperone in parasite morphogenesis, cytoskeletal remodeling during
433 stationary growth phase, motility, and infectivity. How LdCyP40 carries out its parasite-
434 specific functions, and whether they depend on CyP40 isomerase and/or (co-)chaperone
435 activities remains to be elucidated. In other organisms, CyP40 exerts its function mainly
436 through binding to HSP90 (Li *et al.*, 2011). There are several lines of evidence that CyP40
437 functions in *Leishmania* may not follow this established model as isolation of HSP90
438 complexes by anti-STI1 immuno-precipitation from *L. donovani* promastigotes and axenic
439 amastigotes did not reveal LdCyP40 (Morales *et al.*, 2010), although both co-chaperones can
440 bind HSP90 simultaneously in other organisms (Li *et al.*, 2011). In addition, while the
441 LdCyP40 PPIase domain is highly conserved, the TPR domain underwent substantial
442 evolutionary modification (Yau *et al.*, 2010), which may impact on LdCyP40-HSP interactions.
443 Future studies applying structure/function analyses to assess LdCyP40 isomerase and
444 chaperone activities, combined with pull down assays and native electrophoresis, will elucidate
445 the roles of the LdCyP40 PPIase and TPR domains in *L. donovani* differentiation, virulence and
446 stress protein interaction.

447

448

449 **Experimental procedures**

450 **Ethics statement.** All animals were handled according to institutional guidelines of the Central
451 Animal Facility of the Institut Pasteur (Paris, France) and experiments were performed in
452 accordance with protocols approved by the animal Experimentation Ethics Committee of the
453 Institut Pasteur (permit #03–49) and the veterinary service of the French Ministry of
454 Agriculture (number B-75-1159, 30 May 2011). The animals were housed and handled in
455 accordance with good animal practice as defined by FELASA (www.felasa.eu/guidelines.php).

456
457 **Mice, macrophages and parasites.** Wild-type C57BL/6 mice were purchased from Charles
458 River, and were kept and treated according to the institutional guidelines for animal
459 experiments. Bone marrow-derived macrophages (BMMs) were prepared from the femurs of
460 6 – 8 weeks old female mice as described (Forestier *et al.*, 2011). *Leishmania donovani* strain
461 1SR (MHOM/SD/62/1SR) was maintained at 25°C, pH 7.4 in supplemented M199 medium
462 (Kapler *et al.*, 1990; Hubel *et al.*, 1997). Axenic differentiation of promastigotes was performed
463 as described (Goyard *et al.*, 2003; Morales *et al.*, 2008).

464
465 **Multiple sequences analysis.** The putative cyclophilin 40 protein sequences of human, mouse,
466 bovine, yeast and several trypanosomatids, including *L. major*, *L. infantum*, *L. braziliensis*, *T.*
467 *brucei* and *T. cruzi*, were retrieved from the NCBI (<http://www.ncbi.nlm.nih.gov/protein/>) and
468 TriTrypDB databases (<http://tritrypdb.org/tritrypdb/>) by Blast search with algorithm blastp
469 using *L. major* cyclophilin 40 (LmjF35.4770) as a query. The retrieved sequences were aligned
470 with ClustalW 2.0.12 and the aligned data were used to build a neighbour-joining tree and to
471 cluster the CyP40s, using the built-in programs of Geneious version 4.8 (Larkin *et al.*, 2007;
472 Kearse *et al.*, 2012; <http://www.geneious.com>). Matrix Blosum62 was applied as the scoring

473 rule for amino acid substitution (Henikoff and Henikoff, 1993). Sequence alignments with
474 Expect (E) values less than 10^{-5} were considered significant.

475
476 **Generation of *L. donovani* *cyp40*^{-/-} mutants by gene replacement.** Null mutant parasites
477 were generated by sequential replacement of the endogenous *CYP40* alleles using two targeting
478 constructs comprising puromycin and bleomycin resistance genes flanked by approximately
479 1000 bp of the 5' and 3'UTRs of the *L. infantum* *CYP40* gene (GeneDB accession number
480 LinJ.35.4830) that were PCR amplified from *L. infantum* genomic DNA (strain
481 MHOM/FR/91/LEM2259). Genomic DNA of parasites was extracted with Genra Systems
482 Puregene Tissue Core Kit A (Qiagen) according to the manufacturer's instruction.

483 For subsequent cloning of the 5'UTR, primer pairs CYP40-5'UTR-fwd
484 (GGGGAATTCATTTAAATGAGATGCGGTAGATGTCCTG) and CYP40-5'UTR-rev
485 (GGGGGTACCTGCGTGCGTGTAGGTCTAC) added EcoRI and SwaI sites (underlined) to
486 the 5'-end, and a KpnI site to the 3'-end. For cloning of the 3'UTR, primer pairs CYP40-
487 3'UTR-fwd (GGGGGATCCGTTGCGCCTGCCGGACAGAAC) and CYP40-3'UTR-rev
488 (CCCAAGCTTATTTAAATGAGTGAGACGTGCACGCAAC) added BamHI site to the 5'-
489 end, and HindIII and SwaI sites to the 3'-end. The amplified fragments were digested with
490 EcoRI/KpnI and BamHI/HindIII and ligated into pUC19 vector digested with the same enzyme
491 pairs yielding the constructs pUC-CYP40-5'UTR and pUC-CYP40-3'UTR. Next, the cloned
492 5'UTR fragment was liberated by EcoRI and KpnI digestion, ligated into pUC-CYP40-3'UTR
493 digested with the same enzyme pair yielding the construct pUC-CYP40-5'3'UTR. For the
494 construction of the final targeting constructs, the antibiotic resistance genes *PAC* and *BLE* were
495 isolated from pUC-PAC and pUC-BLE after digestion with KpnI and BamHI and ligated into
496 pUC-CYP40-5'3'UTR digested with the same enzymes, yielded the final constructs pUC-
497 CYP40-5'PAC3' and pUC-CYP40-5'BLE3' used for *Leishmania* *CYP40* gene replacement.

498 For genetic complementation of the CYP40 null mutant, an “add-back” line was
 499 established using a knock-in strategy. The *CYP40* open reading frame was PCR amplified using
 500 primers CYP40-5’Kpn (GGGGGTACCATGCCGAACACATACTGC) and CYP40-3’BglII
 501 (GGGAGATCTTCACGAGAACATCTTCTTG), adding KpnI and BglII sites (underlined) to
 502 the 5’- and 3’-ends of the *LmCYP40*, respectively. The amplified fragment was digested with
 503 these enzymes, ligated into pUC-CYP40-3’UTR digested with KpnI and BamHI yielding the
 504 construct pUC-CYP40+3’UTR. The cloned CYP40+3’UTR was liberated by digestion with
 505 Acc65I and SwaI, the 5’-protruding end of the digested fragment was filled-in with Klenow
 506 fragment, and cloned into XbaI/BglII digested and blunt ended vector pIRmcs3+ (Hoyer *et al.*,
 507 2004) yielding the final construct pIR-CYP40 used for integration into the small ribosomal
 508 subunit (SSU) locus of the *cyp40*^{-/-} genome.

509 The plasmids were extracted from transformed *E. coli* DH5 α , purified using CsCl
 510 continuous gradient centrifugation and linearized with SwaI. The targeting fragments were
 511 separated by agarose electrophoresis, purified and transfected into logarithmic promastigotes
 512 by electroporation as described (Spath *et al.*, 2000; Ommen *et al.*, 2009). Integration of gene
 513 replacement constructs was verified by PCR using the primer pairs: (P1,
 514 CATTGGCGCTTTTCATGC; P2, ATTACATCAGACGTAATCTG; P3,
 515 TGGAAAGTGCTACCCTGGTACGTC; P4, GTGGGCTTGTACTCGGTC; P5,
 516 GGAACGGCACTGGTCAAC). PCR products were analyzed by agarose gel electrophoresis.

517
 518 **Site-directed mutagenesis.** Cloned *L. major* *CYP40* in the construct pUC-CYP40+3’UTR was
 519 used as template for site-directed mutagenesis that is based on a modified PCR (Hombach *et*
 520 *al.*, 2013). The template was amplified by PCR using the following phosphorylated
 521 oligonucleotide pairs (mutation sites were underlined) to introduce the mutation: CYP40-
 522 S274A-fwd (GCAGTGGGCGGAGGCTCGCCACACGGCGTC) and CYP40-S274-rev

523 (TGGAGCTTGATGGCGCACATTG). The PCR products were ligated and used to transform
524 competent *E. coli* DH5 α (Invitrogen). Plasmids were extracted and purified for DNA
525 sequencing to verify the mutation.

526

527 **Cell counting.** The cell density of parasite cultures were determined every 24 hours either
528 using a CASY cell counter (Schärfe System) or microscopically by counting 2% (w/v)
529 glutaraldehyde fixed cells loaded into a Neubauer-improved cell counting chamber
530 (Marienfeld).

531

532 **Macrophage infection assays.** Isolation and differentiation of BMMs were performed as
533 described (Forestier *et al.*, 2011). The mature BMMs were treated with 20 mM EDTA for
534 detachment. The dislodged cells were resuspended in complete RPMI medium and plated
535 overnight in 24-well plates containing sterile 12-mm glass coverslips at a cell density of 1×10^5
536 cells/well. *L. donovani* promastigotes cultured for 6 days until stationary-phase ($8 - 10 \times$
537 10^7 /ml), or axenic amastigotes from logarithmic growth phase ($1 - 5 \times 10^7$ /ml) were washed
538 three times with plain RPMI medium and once with infection medium (0.7% BSA, 25 mM
539 HEPES [pH 7.4] in plain RPMI medium), incubated with BMMs at 37°C with 5% CO₂ for 2
540 hours at a multiplicity of infection of 10 parasites per host cell. Extracellular parasites were
541 then removed by washing the coverslips extensively with PBS and transfer of the cover slip
542 into new 24-well plates containing 1 ml of fresh complete RPMI medium per well. This
543 washing procedure was repeated daily until 5 days post infection. The plates were incubated for
544 up to 5 days at 37°C with 5% CO₂ during the experiment.

545

546 **Analysis of intracellular parasite burden.** Coverslips of quadruplicate experiments were
547 collected at 0, 24 and 48 hours post infection, washed once with PBS and then fixed with 4%

548 (w/v) paraformaldehyde for 15 min at room temperature. After three further washes with PBS
549 and one wash with ddH₂O, the coverslips were mounted with Mowiol medium containing
550 nuclear dye Hoechst 33342 (Invitrogen). At least 100 macrophages were imaged per coverslip
551 using Axioplan 2 wide field light microscope with the Apotome module (Carl Zeiss). Number
552 of parasites and macrophages was estimated counting host cell and parasite nuclei using ImageJ
553 (National Institute of Health, US) using a predefined pixel range for each cell type (400 to
554 infinity pixels, macrophages; 0 to 150 pixels, parasites; 100 to 200 pixels, CFSE labeled
555 parasites in case of mixed infection assay).

556
557 **Microscopic analyses.** *Giemsa staining analysis.* Parasites (1×10^6) were settled on poly-L-
558 lysine coated glass slides and air-dried overnight. The dried cells were fixed with methanol and
559 stained with Giemsa solution (Sigma) for 10 min. After rinsing with water and air-drying, the
560 slides were mounted with Immersol 518N (Carl Zeiss) and observed under an Axioplan 2 wide
561 field light microscope (Carl Zeiss). The acquired images were analyzed by Zeiss Axiovision
562 release 4.7 (Carl Zeiss) or Openlab v3.0 (Improvision).

563 *Scanning electron microscopy.* Parasites were washed twice in ice-cold PBS and then
564 fixed with 2% (w/v) glutaraldehyde (Sigma) in PBS with 0.1 M sodium cacodylate (pH 7.2).
565 Briefly, the fixed cells were treated with 1% (w/v) OsO₄ and dehydrated followed by critical-
566 point drying (CPD 7501, Polaron) and coated with gold powder (Ion Beam Coater 681, Gatan).
567 Samples were visualized with scanning electron microscope SEM 500 (Philips). For
568 cytoskeleton analysis, cells were treated with 1% Triton X-100 at 4°C in PBS for 10 minutes to
569 strip the plasma membrane and visualize the cytoskeleton. The samples were then washed
570 twice in PBS, fixed in glutaraldehyde and processed for scanning electron microscopy in
571 standard conditions as described (Absalon *et al.*, 2008).

572 *Transmission electron microscopy.* Parasites were washed twice in ice-cold PBS and
 573 then fixed with 2% (v/v) glutaraldehyde (Sigma) in PBS with 0.1 M sodium cacodylate (pH
 574 7.2). The fixed cells were post-fixed in 1% (w/v) OsO₄ and then dehydrated with increasing
 575 ethanol concentrations (70–100%) and embedded in EPON epoxy resin (Hexion Speciality
 576 Chemicals). Ultrathin sections (~70 nm) were prepared using an Ultramicrotome (Ultra Cut E;
 577 Reichert/Leica) and stained with uranyl acetate and lead citrate. Sections were analyzed using
 578 the Tecnai Spirit TEM (FEI).

579
 580 **Annexin V-FITC assay.** Parasites (2×10^7 cells) were washed and resuspended in 100 μ l of
 581 binding buffer containing 100 μ g/ml of FITC conjugated annexin V (a gift from Dr. Aude
 582 Foucher, Photeomix, Paris), 1 μ g/ml of PI, 10 mM HEPES (pH 7.4), 140 mM NaCl and 5 mM
 583 CaCl₂. The suspensions were incubated at room temperature for 10 min in the dark. The stained
 584 cells were subjected to FACS analysis ($\lambda_{\text{ex}} = 488$ nm; $\lambda_{\text{em}} = 515$ nm [FITC] and 617 nm [PI])
 585 with a FACSCalibur™ (BD Biosciences). 10,000 events were analyzed using FlowJo 8.7 (Tree
 586 Star).

587
 588 **SYBR Green-based semi-quantitative RT-PCR.** SHERP cDNA was amplified using forward
 589 primer CGACAAGATCCAGGAGCTGAAGGAC and reversed primer
 590 CCTTGATGCTCTCAACCGTGCTG). Beta actin cDNA was amplified as reference gene to
 591 calculate relative expression levels of SHERP mRNA.

592
 593 **Motility analysis.** For each condition, at least 3 movies were recorded (500 frames at 33 ms of
 594 exposure for 16 s movies). Samples were observed in their respective culture media (cell
 595 density of about 5×10^6 cells/ml in logarithmic phase or 10^7 cells/ml in stationary phase) under
 596 a 10 \times objective of an inverted DMI4000 microscope (Leica). Cells were filmed using a

597 numeric camera Photometrics Evolve 512 (Photometrics). Movies were converted with the
598 MPEG Streamclip V1.9b3 software (Squared 5) and analyzed with the ICY software
599 (<http://www.bioimageanalysis.org/>). For each movie, at least 255 cells were simultaneously
600 tracked in silico. Mean speeds (in $\mu\text{m/s}$) were calculated from instant velocity data transferred
601 and compiled in Microsoft Excel. Statistical analyses were performed in the KaleidaGraph
602 V4.0 software (Synergy Software). Data were first filtered (number of spot detections > 3 and
603 mean speed $< 100 \mu\text{m/s}$) to exclude false tracks (non-*Leishmania* objects, dead cells and/or
604 attached cells). An ANOVA test was then performed with Tukey ad-hoc post-tests at 0.5 for
605 intergroup comparisons ($p < 0.0001$).

606
607 ***Leishmania* phosphoprotein enrichment.** Promastigotes, axenic amastigotes, and splenic
608 amastigotes derived from *Leishmania* infected hamsters, were centrifuged at $1000 \times g$ at 4°C
609 for 10 min. Pellets were washed twice with plain M199 medium, then resuspended in lysis
610 buffer (150 mM NaCl, 50 mM Tris-HCl pH 7.4, 1% Triton X-100, 1% benzonase, and protease
611 inhibitor cocktail [Roche]) and lysed at 4°C for 30 min with vortexing every 10 min. The lysate
612 was then sonicated on ice for 5 min (10 seconds pulse with a 20 seconds pause) using Bioruptor
613 (Diagenode). Cell debris was removed by brief centrifugation. Protein concentration of lysates
614 was estimated by RC DC protein assay (Bio-rad) and adjusted to 0.1 mg protein/ml with lysis
615 buffer. Phosphoprotein was enriched using the Phosphoprotein purification kit (Qiagen)
616 according to the manufacturer's instructions. Briefly, 2.5 mg of total protein were loaded to the
617 equilibrated columns. Unbound proteins were removed by washing the column with 6 ml of
618 lysis buffer. Bound phosphorylated proteins were eluted with 2 ml elution buffer and
619 concentrated using Amicon Ultra-0.5 ml centrifugal filters with Ultracel® 10K membrane
620 (Millipore).

621

622 **Phosphopeptide identification.** Cell lysate extracted from transgenic *L. donovani* expressing
623 Strep::CyP40 (refer to supporting information) was separated by SDS-PAGE. Separated
624 Strep::CyP40 was trypsin-digested and diluted in loading buffer (80% ACN, 5% TFA). The
625 sample was then processed for LC-ESI-MS/MS analysis to identify phosphorylation sites, as
626 described (Morales *et al.*, 2010). Briefly, digested protein was diluted in loading buffer (80%
627 ACN, 5% TFA) and loaded on TiO₂ microcolumns. After two washing steps in 10 μ l loading
628 buffer and 60 μ l buffer 2 (80% ACN, 1% TFA), phosphopeptides were eluted using 10 μ l
629 NH₄OH (pH 12), dried, then resuspend in 10 μ l of 0.1% formic acid before analyzing with a Q-
630 TOF mass spectrometer (Maxis; Bruker Daltonik GmbH, Bremen, Germany), interfaced with a
631 nano-HPLC U3000 system (Thermo Scientific, Waltham, USA). Samples were concentrated
632 with a pre-column (Thermo Scientific, C18 PepMap100, 300 μ m \times 5 mm, 5 μ m, 100 Å) at a
633 flow rate of 20 μ L/min using 0.1% formic acid. After pre-concentration, peptides were
634 separated with a reversed-phase capillary column (Thermo Scientific, C18 PepMap100, 75 μ m
635 \times 250 mm, 3 μ m, 100 Å) at a flow rate of 0.3 μ L/min using a two-step gradient (8 % to 28 %
636 acetonitrile in 40 min then 28 % to 42 % in 10 min), and eluted directly into the mass
637 spectrometer. Proteins were identified by MS/MS by information-dependent acquisition of
638 fragmentation spectra of multiple charged peptides and MS/MS raw data were analysed using
639 Data Analysis software (Bruker Daltonik GmbH, Bremen, Germany) to generate the peak lists.
640 The *L. major* database from GeneDB was searched using MASCOT software (Matrix Science,
641 London, UK) with the following parameters: trypsin cleavage, one missed cleavage sites
642 allowed, carbamidomethylation set as fixed modification, 10 ppm mass tolerance for MS, and
643 0.05 Da for MS/MS fragment ions. Phosphorylation (ST), Phosphorylation (Y) and oxidation
644 (M) were allowed as variable modifications. All phosphorylated peptides were first checked for
645 the presence of the major fragment ion $[MH-H_3PO_4]^+ = MH - 98$ Da corresponding to the loss

646 of the phosphate moiety and identified positively by MASCOT. In addition, all MS/MS spectra
647 were carefully checked manually for assignment of phosphorylation sites.

648
649 **Western blot analysis.** Samples in 1× Laemmli buffer were separated by 10% SDS-PAGE and
650 then transferred to PVDF membranes. Rabbit anti-CyP40 antiserum (1:20000 dilution, Yau *et*
651 *al.*, 2010), mouse anti-A2 antibody (clone C9, 1:50 dilution, Zhang *et al.*, 1996), mouse anti-
652 LPG antibody (clone CA74E, 1:20000 dilution, Tolson *et al.*, 1994), mouse anti- α -tubulin
653 antibody (clone B-5-1-2, 1:20000 dilution, Sigma), mouse anti- β -tubulin antibody (clone
654 KMX, 1:100 dilution, Absalon *et al.*, 2007), goat anti-mouse HRP conjugated antibody
655 (1:20000 dilution, Thermo Scientific) and goat anti-rabbit HRP conjugated antibody (1:20000
656 dilution, Thermo Scientific) were used to probe the membrane. SuperSignal West Pico
657 chemiluminescent substrate (Thermo Scientific) was added to the membranes and
658 chemiluminescent signals were revealed on X-ray films.

659
660 **Statistical analysis.** Numerical data were expressed as mean \pm standard deviation. Mann-
661 Whitney U test was used to compare the significance between specific groups and $p < 0.05$ was
662 considered as statistically significant. All statistical analysis was performed using either Excel
663 2003 (Microsoft) or Prism 5.0 (GraphPad).

664
665 **Acknowledgments**
666 We thank Dirk Schmidt-Arras (University of Kiel), Gabi Ommen, Mareike Chrobak and
667 Christel Schmetz (Bernhard Nocht Institute, Hamburg) for discussion, Eric Prina for critical
668 reading of the manuscript, Claire Forestier and Evie Melanitou (Institut Pasteur) for advices on
669 macrophage experiment, Emanuelle Perret from the Institut Pasteur Imaging platform for
670 advice on fluorescence microscopy, and Abdelkader Namane from the Institut Pasteur

671 Proteomics platform for protein determination. This work was supported by the Institut Pasteur,
672 Réseau International des Instituts Pasteur, Centre Nationale de Recherche Scientifique, the 7th
673 Framework Programme of the European Commission through a grant to the LEISHDRUG
674 Project (223414), the Fondation de Médicale Recherche and Deutscher Akademischer
675 Austausch Dienst, and the French Government's Investissements d'Avenir program:
676 Laboratoire d'Excellence 'Integrative Biology of Emerging Infectious Diseases' (grant no.
677 ANR-10-LABX-62-IBEID).

678

679

680

681 **Figure legends**

682 **Fig 1. *L. donovani* CyP40 is a conserved chaperone and shows amastigote-specific**
683 **phosphorylation.** (A) *Amino acid sequence analysis of Leishmania CyP40.* Multiple alignment
684 of CyP40 amino acid sequences of mammal (human, mouse and bovine), trypanosomatid
685 (*Leishmania* and *Trypanosoma*) and yeast was performed using ClustalW as described in
686 experimental procedures. CLD/PPIase (cyclophilin-like domain/PPIase) and TPR domains are
687 indicated. Degree of residue conservation is represented by the colour code (green, 80-100%
688 conserved; yellow, 30-80% conserved; red, 10-30% conserved). *, key residues for cyclosporin
689 A binding and PPIase activity; ^, key residues for chaperone function; Δ, key residues for
690 HSP90 binding. Accession numbers: M.mus, NP_080628.1; H.sap, NP_005029.1; B. tau,
691 NP_776578.1; S.cer, NP_013317.1; T.cru, TcCLB.506885.400; T.bru, Tb927.9.9780; L.bra,
692 LbrM34.4730; L.mex, LmxM34.4770; L.inf, LinJ35.4830; L.maj, LmjF35.4770. (B) *Western*
693 *blot analysis.* Phosphoproteins of *in vitro* cultivated *L. donovani* promastigote (pro), axenic
694 amastigote (ama, ax), and amastigotes harvested from infected hamster spleen (sp) were
695 enriched using a Phosphoprotein purification kit (Qiagen). Total and phosphoprotein

696 extracts were analyzed by Western blotting using anti-CyP40 antiserum and anti- α -tubulin
 697 antibody for normalization.

698

699 **Fig. 2. CyP40 null mutant parasites are viable in culture.** (A) *Targeted replacement and*
 700 *add-back strategies.* Targeting constructs comprising bleomycin (*BLE*) and puromycin (*PAC*)
 701 resistance genes flanked by the *CYP40* 5' and 3' untranslated regions (UTRs) were used for
 702 deletion of the genomic *CYP40* alleles. A targeting construct containing the nourseothricin
 703 resistance gene (*SAT*) and the *Leishmania major CYP40* open reading frame (ORF) flanked by
 704 the *L. major* small ribosomal subunit homology regions (*LmSSU*) were used for restoring
 705 CyP40 expression in the *cyp40*^{-/-} parasites. Primers specific for amplifying *CYP40* (P1/P4), the
 706 resistance genes *PAC* (P2/P4) and *BLE* (P3/P4), and the *SSU* locus (P1/P5) are indicated. (B)
 707 *Validation of homologous recombination events by PCR analysis.* Genomic DNA of wild-type
 708 (WT), heterozygous CyP40 null mutant (-/+), homozygous CyP40 null mutant (-/-) and CyP40
 709 add-back (-/-/+) was subjected to diagnostic PCR analysis using the indicated primer pairs
 710 (P_xP_y) to amplify the endogenous CyP40 ORF (*CYP*), the *CYP40* ORF integrated into the
 711 ribosomal locus (*SSU*), and the bleomycin (*BLE*) and puromycin (*PAC*) resistance genes. (C)
 712 *Western blot analysis.* Total protein from wild-type (WT) and CyP40 null mutant (-/-) and add-
 713 back (-/-/+) were extracted and analyzed by western blotting using anti-CyP40 (CyP, upper
 714 panel) and anti- α -tubulin antibodies (Tub, lower panel). The molecular weight of marker
 715 proteins in kDa is indicated.

716

717 **Fig. 3. Stationary *cyp40*^{-/-} promastigotes show altered morphology.** (A) *Morphological*
 718 *analysis.* Promastigotes of wild-type (WT), *cyp40*^{-/-} (clones 4 and 5) and the respective *cyp40*^{-/-}
 719 */+ clones* from logarithmic and stationary growth phase were stained with Giemsa and
 720 analyzed using a light microscope (Leica) controlled by OpenLab v3.0 (Improvision). Scale bar

721 represents 10 μm . (B, C) *Electron microscopy analysis*. Promastigotes from stationary growth
 722 phase were fixed and processed for either scanning (B) or transmission EM (C) as described in
 723 Materials and Methods. Scale bar represents 10 μm in the scanning EM panels and 500 nm in
 724 the transmission EM panels. (D) *Cell viability determination*. Stationary promastigotes of wild-
 725 type (WT) and *cyp40*^{-/-} (-/-) from 6 days cultures were stained with propidium iodide (PI, 1
 726 $\mu\text{g/ml}$) and annexin V-FITC (1 $\mu\text{g/ml}$) for 10 min, and respective fluorescence intensities were
 727 analyzed by FACS. Numbers at the lower-right quadrant represent percentage of apoptotic cells
 728 (PI-, Annexin V-FITC+), while numbers at the upper-right quadrant represent percentage of
 729 dead cells (PI+, Annexin V-FITC+).

730
 731 **Fig 4. Growth characterization of Cyp40 null mutant promastigotes.** (A) *In vitro growth*
 732 *curve of cyp40*^{-/-} mutants. Promastigotes of wild-type (WT), *cyp40*^{-/-} (-/-) and *cyp40*^{-/+} (-/+) were
 733 cultured at 25°C, pH 7.4 for 120 hours. Aliquots of culture were collected every 24 hours
 734 and cell density was measured with a CASY cell counter. (B) *Western blot analysis of LPG*
 735 *expression*. 5×10^6 wild-type or *cyp40*^{-/-} parasites from logarithmic (log) or stationary (stat)
 736 cell culture were subjected to western blot analysis using anti-LPG antibody. (C) *RT-PCR of*
 737 *SHERP expression*. Total RNA of the wild-type (black), *cyp40*^{-/-} (white) and *cyp40*^{-/+} (gray)
 738 were extracted, reverse transcribed, and amplified with SHERP specific primer. β -tubulin was
 739 amplified with specific primers as reference gene. Relative expression levels of SHERP mRNA
 740 was analyzed using semi-quantitative RT-PCR.

741
 742 **Fig. 5. Analyses of motility and cytoskeleton of stationary phase *cyp40*^{-/-} promastigote.** (A,
 743 B) *Motility analysis*. Motility tracks were established for logarithmic (log) and stationary phase
 744 (stat) wild-type (WT), *cyp40*^{-/-} (-/-) and *cyp40*^{-/+} (-/+) promastigotes. For each condition, at
 745 least 3 movies were recorded for the simultaneous *in silico* tracking of at least 255 cells per

746 movie. Mean speed (in $\mu\text{m/s}$) was calculated from instant velocity data and graphically
 747 represented in left panel with SD bars. *ANOVA test, $p < 0.0001$. $n=735$ for WT Log and 737
 748 for WT Stat, $n=746$ for -/- Log and 747 for -/- Stat, $n=741$ for -/-/+ Log and 742 for -/-/+ Stat.
 749 Characteristic tracks are shown in Fig. 5B. (C) *Flagellar ultrastructure of stationary WT and*
 750 *cyp40-/- promastigotes*. Scale bar represents 100 nm. (D) *Cytoskeleton analysis*. Wild-type
 751 (WT) and *cyp40-/- (-/-)* stationary promastigotes were treated with 1% Triton X-100 at 4°C in
 752 PBS for 10 minutes to strip the plasma membrane and visualize the parasite cytoskeleton.
 753 Samples were washed twice in PBS, fixed and processed for scanning electron microscopy as
 754 described (Absalon *et al.*, 2008). Scale bar represents 100 nm. (E) *Western blot analysis of*
 755 *HSPs and tubulin expression*. Crude lysate of 5×10^6 parasites obtained from logarithmic (log)
 756 or stationary (stat) cultures were boiled directly in Laemmli buffer and separated on NuPAGE
 757 4-12% gel, and transferred to PVDF membranes. The membranes were then incubated with
 758 mouse monoclonal IgG clone B-5-1-2 antibody for α -tubulin or monoclonal IgG clone KMX
 759 antibody for β -tubulin, and subsequently incubated with anti-mouse IgG conjugated with HRP.
 760 Signals were revealed by chemiluminescence after addition of substrate. The molecular weight
 761 of marker proteins in kDa is indicated.

762

763 **Fig. 6. Intracellular survival and axenic differentiation of the *cyp40-/-* null mutants.** (A)

764 *Macrophage infection assay*. BMMs from C57BL/6 mice were infected with stationary phase
 765 promastigotes of *L. donovani* wild-type (WT, O), *cyp40-/-* (clone 4, □, and 5, ■) or *cyp40-/-/+*
 766 (Δ) for 2 hours, and parasite burden was analyzed at 0, 24 and 48 hours post-infection by
 767 nuclear staining with Hoechst 33342 and fluorescence microscopy. Results are representative
 768 of three triplicate experiments with standard deviation denoted by the bars is shown. (B) In
 769 vitro growth curve of *cyp40-/-* axenic amastigotes. Promastigotes of wild-type (WT), *cyp40-/-*
 770 (*-/-*) and *cyp40-/-/+ (-/-/+)* were induced for axenic differentiation at 37°C, pH 5.5 for 72 hours,

771 and amastigote growth was monitored following inoculation of 2×10^6 axenic amastigotes into
 772 fresh medium and daily determination of cell density with a CASY cell counter. (C) *A2 marker*
 773 *protein expression analysis*. Extracts from wild-type (WT), *cyp40*^{-/-} (-/-) and *cyp40*^{-/+} (-/+)
 774 axenic amastigotes 72 hours after incubation under differentiation-inducing conditions were
 775 subjected to western blot analysis using an axenic amastigote marker A2-specific monoclonal
 776 antibody (upper panel). Equal loading was controlled by Coomassie staining (lower panel). The
 777 molecular weight of marker proteins in kDa is indicated.

778

779 **Fig 7. Effect of phosphorylation of CyP40 on *Leishmania* intracellular survival.** (A, B)
 780 *Phosphorylation site identification*. (A) Peptide 270LQQWSEAR277 (m/z 1098.49) was
 781 identified in LC-ESI-MS/MS analysis of *L. major* Strep::CyP40 peptides after tryptic digestion
 782 and TiO₂ enrichment and Ser274 was identified as a phosphorylated residue. *, fragment ions
 783 arising from loss of ammonia (-17 Da); pS, phosphorylated serine. (B) *Multiple sequence*
 784 *alignment of L. major CyP40 phosphoresidue*. Sequence segments encompassing CyP40
 785 phosphorylation site of mouse, human, bovine, yeast, two *Trypanosoma* (*T. cruzi*, *T. brucei*),
 786 four *Leishmania* species (*L. braziliensis*, *L. mexicana*, *L. infantum*, *L. major*) were analyzed
 787 with ClustalW. The phospho-residue Ser274 of *L. major* CyP40 is marked by an asterisk (*).
 788 (C) *Analysis of the CyP40-S274A add-back line by western blotting*. Total protein (left panel)
 789 from wild-type (WT) and CyP40 null mutant (-/-) and Cyp40-WT and CyP40-S274A add-back
 790 lines (-/+ and S274A, respectively), and enriched phosphoprotein extracts (right panel) of
 791 axenic amastigotes of *L. donovani* wild-type (WT) and *cyp40*^{-/+S274A} (S274A) were
 792 analyzed. As background control of the phosphoprotein enrichment, 2 mg of the WT total
 793 extract were first treated with 8000 units of lambda phosphatase (λPP) for 2 hours at 30°C. The
 794 λPP-treated sample was then subjected to phosphoprotein enrichment. The total and
 795 phosphoprotein (Phospho) extracts of the parasites were analyzed by Western blotting using

796 anti-CyP40 antiserum and anti- α -tubulin antibody. The molecular weight of marker proteins in
797 kDa is indicated. (D) *Macrophage infection assay*. BMMs from C57BL/6 mice were infected
798 for 2 hours with stationary phase promastigotes of *L. donovani* wild-type (WT, ○), *cyp40*^{-/-} (-/-
799 , □) or CyP40-WT and CyP40-S274A add-backs (respectively -/-/+, Δ and -/-/+S/A, ▼) and
800 parasite burden was at 0, 24 and 48 hours post-infection by nuclear staining with Hoechst
801 33342 and fluorescence microscopy. Result is presented as percentage infected BMMs (left
802 panel, one representative triplicate experiment with standard deviation denoted by the bars is
803 shown), and number of parasites per 100 BMMs at 48 hours post-infection (right panels, results
804 of one representative triplicate experiment with standard deviation denoted by the bars is
805 shown).

806

807

808

809 **References**

- 810 Absalon, S., Kohl, L., Branche, C., Blisnick, T., Toutirais, G., Rusconi, F., Cosson, J.,
811 Bonhivers, M., Robinson, D., and Bastin, P. (2007) Basal body positioning is controlled by
812 flagellum formation in *Trypanosoma brucei*. *PLoS ONE* **2**: e437.
- 813 Absalon, S., Blisnick, T., Bonhivers, M., Kohl, L., Cayet, N., Toutirais, G., *et al.* (2008)
814 Flagellum elongation is required for correct structure, orientation and function of the
815 flagellar pocket in *Trypanosoma brucei*. *J Cell Sci* **121**: 3704-3716.
- 816 Barak, E., Amin-Spector, S., Gerliak, E., Goyard, S., Holland, N. and Zilberstein, D. (2005)
817 Differentiation of *Leishmania donovani* in host-free system: analysis of signal perception
818 and response. *Mol Biochem Parasitol* **141**: 99-108.
- 819 Barik, S. (2006) Immunophilins: for the love of proteins. *Cell Mol Life Sci* **63**: 2889-2900.

- 820 Bates, P.A., and Tetley, L. (1993) *Leishmania mexicana*: Induction of metacyclogenesis by
821 cultivation of promastigotes at acidic pH. *Exp Parasitol* **76**: 412–423.
- 822 Brasseur, A., Rotureau, B., Vermeersch, M., Blisnick, T., Salmon, D., Bastin, P., Pays, E.,
823 Vanhamme, L., and Pérez-Morga, D. (2013) *Trypanosoma brucei* FKBP12 differentially
824 controls motility and cytokinesis in procyclic and bloodstream forms. *Euk Cell* **12**: 168–181.
- 825 Chambraud, B., Belabes, H., Fontaine-Lenoir, V., Fellous, A. and Baulieu, E.E. (2007) The
826 immunophilin FKBP52 specifically binds to tubulin and prevents microtubule formation.
827 *FASEB J* **21**: 2787-2797.
- 828 Chappell, L.H. and Wastling, J.M. (1992) Cyclosporin A: antiparasite drug, modulator of the
829 host-parasite relationship and immunosuppressant. *Parasitology* **105 Suppl**: S25-40.
- 830 Cunningham, M.L., Titus, R.G., Turco, S.J. and Beverley, S.M. (2001) Regulation of
831 differentiation to the infective stage of the protozoan parasite *Leishmania major* by
832 tetrahydrobiopterin. *Science* **292**: 285-287.
- 833 da Silva, R. and Sacks, D.L. (1987) Metacyclogenesis is a major determinant of *Leishmania*
834 promastigote virulence and attenuation. *Infect Immun* **55**: 2802-2806.
- 835 Drummelsmith, J., Brochu, V., Girard, I., Messier, N. and Ouellette, M. (2003) Proteome
836 mapping of the protozoan parasite *Leishmania* and application to the study of drug targets
837 and resistance mechanisms. *Mol Cell Proteomics* **2**: 146-155.
- 838 Duina, A.A., Marsh, J.A. and Gaber, R.F. (1996) Identification of two CyP-40-like cyclophilins
839 in *Saccharomyces cerevisiae*, one of which is required for normal growth. *Yeast* **12**: 943-952.
- 840 Forestier, C.L., Machu, C., Loussert, C., Pescher, P. and Spath, G.F. (2011) Imaging host cell-
841 *Leishmania* interaction dynamics implicates parasite motility, lysosome recruitment, and
842 host cell wounding in the infection process. *Cell Host Microbe* **9**: 319-330.
- 843 Galat, A. (2003) Peptidylprolyl cis/trans isomerases (immunophilins): biological diversity--
844 targets--functions. *Curr Top Med Chem* **3**: 1315–1347.

- 845 Galigniana, M.D., Radanyi, C., Renoir, J.M., Housley, P.R., and Pratt, W.B. (2001) Evidence
 846 that the peptidylprolyl isomerase domain of the hsp90-binding immunophilin FKBP52 is
 847 involved in both dynein interaction and glucocorticoid receptor movement to the nucleus. *J*
 848 *Biol Chem* **276**: 14884–14889.
- 849 Galigniana, M.D., Morishima, Y., Gallay, P.A., and Pratt, W.B. (2004) Cyclophilin-A is bound
 850 through its peptidylprolyl isomerase domain to the cytoplasmic dynein motor protein
 851 complex. *J Biol Chem* **279**: 55754–55759.
- 852 Gannavaram, S., and Debrabant, A. (2012) Programmed cell death in *Leishmania*: biochemical
 853 evidence and role in parasite infectivity. *Front Cell Infect Microbiol* **2**: 95.
- 854 Goyard, S., Segawa, H., Gordon, J., Showalter, M., Duncan, R., Turco, S.J. and Beverley, S.M.
 855 (2003) An *in vitro* system for developmental and genetic studies of *Leishmania donovani*
 856 phosphoglycans. *Mol Biochem Parasitol* **130**: 31-42.
- 857 Hem, S., Gherardini, P.F., Osorio y Fortea, J., Hourdel, V., Morales, M.A., Watanabe, R., *et al.*
 858 (2010) Identification of *Leishmania*-specific protein phosphorylation sites by LC-MS/MS
 859 and comparative genomics analyses. *Proteomics* **10**: 3868-3883.
- 860 Henikoff, S., and Henikoff, J.G. (1993) Performance evaluation of amino acid substitution
 861 matrices. *Proteins* **17**: 49–61.
- 862 Ho, S., Clipstone, N., Timmermann, L., Northrop, J., Graef, I., Fiorentino, D., Nourse, J., and
 863 Crabtree, G.R. (1996) The mechanism of action of cyclosporin A and FK506. *Clin Immunol*
 864 *Immunopathol* **80**: S40–S45.
- 865 Hoffmann, K. and Handschumacher, R.E. (1995) Cyclophilin-40: evidence for a dimeric
 866 complex with hsp90. *Biochem J* **307**: 5-8.
- 867 Hombach, A., Ommen, G., Chrobak, M., and Clos, J. (2012) The Hsp90-Sti1 Interaction is
 868 Critical for *Leishmania donovani* Proliferation in Both Life Cycle Stages. *Cell Microbiol*
 869 (Epub ahead of print)

- 870 Hong, J., Kim, S.T., Tranguch, S., Smith, D.F., and Dey, S.K. (2007) Deficiency of co-
 871 chaperone immunophilin FKBP52 compromises sperm fertilizing capacity. *Reproduction*
 872 **133**: 395–403.
- 873 Hoyer, C., Zander, D., Fleischer, S., Schilhabel, M., Kroener, M., Platzer, M. and Clos, J. (2004)
 874 A *Leishmania donovani* gene that confers accelerated recovery from stationary phase growth
 875 arrest. *Int J Parasitol* **34**: 803-811.
- 876 Hubel, A., Krobitch, S., Horauf, A. and Clos, J. (1997) *Leishmania major* Hsp100 is required
 877 chiefly in the mammalian stage of the parasite. *Mol Cell Biol* **17**: 5987 - 5995.
- 878 Iiki, T., Yoshikawa, M., Meshi, T., and Ishikawa, M. (2012) Cyclophilin 40 facilitates HSP90-
 879 mediated RISC assembly in plants. *EMBO J* **31**: 267–278.
- 880 Kapler, G.M., Coburn, C.M. and Beverley, S.M. (1990) Stable transfection of the human
 881 parasite *Leishmania major* delineates a 30-kilobase region sufficient for extrachromosomal
 882 replication and expression. *Mol Cell Biol* **10**: 1084-1094.
- 883 Kearse, M., Moir, R., Wilson, A., Stones-Havas, S., Cheung, M., Sturrock, S., Buxton, S.,
 884 Cooper, A., Markowitz, S., Duran, C., et al. (2012) Geneious Basic: an integrated and
 885 extendable desktop software platform for the organization and analysis of sequence data.
 886 *Bioinformatics* **28**: 1647–1649.
- 887 Krobitch, S., and Clos, J. (1999) A novel role for 100 kD heat shock proteins in the parasite
 888 *Leishmania donovani*. *Cell Stress Chaperones* **4**: 191–198.
- 889 Kulkarni, M.M., Karafova, A., Kamysz, W., Schenkman, S., Pelle, R., and McGwire, B.S.
 890 (2013) Secreted trypanosome cyclophilin inactivates lytic insect defense peptides and
 891 induces parasite calcineurin activation and infectivity. *J Biol Chem* **288**: 8772–8784.
- 892 Larkin, M.A., Blackshields, G., Brown, N.P., Chenna, R., McGettigan, P.A., McWilliam, H.,
 893 Valentin, F., Wallace, I.M., Wilm, A., Lopez, R., et al. (2007) Clustal W and Clustal X
 894 version 2.0. *Bioinformatics* **23**: 2947–2948.

- 895 Laubach, V.E., Shesely, E.G., Smithies, O. and Sherman, P.A. (1995) Mice lacking inducible
896 nitric oxide synthase are not resistant to lipopolysaccharide-induced death. *Proc Natl Acad*
897 *Sci U S A* **92**: 10688-10692.
- 898 Lee, N., Bertholet, S., Debrabant, A., Muller, J., Duncan, R., and Nakhasi, H.L. (2002)
899 Programmed cell death in the unicellular protozoan parasite *Leishmania*. *Cell Death Differ*
900 **9**: 53–64.
- 901 Li, J., Richter, K. and Buchner, J. (2011) Mixed Hsp90-cochaperone complexes are important
902 for the progression of the reaction cycle. *Nat Struct Mol Biol* **18**: 61-66.
- 903 Mark, P.J., Ward, B.K., Kumar, P., Lahooti, H., Minchin, R.F. and Ratajczak, T. (2001) Human
904 cyclophilin 40 is a heat shock protein that exhibits altered intracellular localization
905 following heat shock. *Cell Stress Chaperones* **6**: 59-70.
- 906 McCaffrey, P.G., Perrino, B.A., Soderling, T.R., and Rao, A. (1993) NF-ATp, a T lymphocyte
907 DNA-binding protein that is a target for calcineurin and immunosuppressive drugs. *J Biol*
908 *Chem* **268**: 3747–3752.
- 909 Miyata, Y., Chambrud, B., Radanyi, C., Leclerc, J., Lebeau, M.C., Renoir, J.M., Shirai, R.,
910 Catelli, M.G., Yahara, I., and Baulieu, E.E. (1997) Phosphorylation of the
911 immunosuppressant FK506-binding protein FKBP52 by casein kinase II: regulation of
912 HSP90-binding activity of FKBP52. *Proc Natl Acad Sci U S A* **94**: 14500–14505.
- 913 Mojtahedi, Z., Clos, J. and Kamali-Sarvestani, E. (2008) *Leishmania major*: Identification of
914 developmentally regulated proteins in procyclic and metacyclic promastigotes. *Exp*
915 *Parasitol* **119**: 422-429.
- 916 Mok, D., Allan, R.K., Carrello, A., Wangoo, K., Walkinshaw, M.D., and Ratajczak, T. (2006)
917 The chaperone function of cyclophilin 40 maps to a cleft between the prolyl isomerase and
918 tetratricopeptide repeat domains. *FEBS Lett* **580**: 2761–2768.

- 919 Morales, M.A., Renaud, O., Faigle, W., Shorte, S.L. and Spath, G.F. (2007) Over-expression of
 920 *Leishmania major* MAP kinases reveals stage-specific induction of phosphotransferase
 921 activity. *Int J Parasitol* **37**: 1187-1199.
- 922 Morales, M.A., Watanabe, R., Laurent, C., Lenormand, P., Rousselle, J.C., Namane, A. and
 923 Spath, G.F. (2008) Phosphoproteomic analysis of *Leishmania donovani* pro- and amastigote
 924 stages. *Proteomics* **8**: 350-363.
- 925 Morales, M.A., Watanabe, R., Dacher, M., Chafey, P., Osorio y Fortea, J., Scott, D.A., *et al.*
 926 (2010) Phosphoproteome dynamics reveal heat-shock protein complexes specific to the
 927 *Leishmania donovani* infectious stage. *Proc Natl Acad Sci U S A* **107**: 8381-8386.
- 928 Oberholzer, M., Langousis, G., Nguyen, H.T., Saada, E.A., Shimogawa, M.M., Jonsson, Z.O.,
 929 Nguyen, S.M., Wohlschlegel, J.A., and Hill, K.L. (2011) Independent analysis of the
 930 flagellum surface and matrix proteomes provides insight into flagellum signaling in
 931 mammalian-infectious *Trypanosoma brucei*. *Mol Cell Proteomics* **10**: M111.010538.
- 932 Ommen, G., Lorenz, S. and Clos, J. (2009) One-step generation of double-allele gene
 933 replacement mutants in *Leishmania donovani*. *Int J Parasitol* **39**: 541-546.
- 934 Parodi-Talice, A., Monteiro-Goes, V., Arrambide, N., Avila, A.R., Duran, R., Correa, A., *et al.*
 935 (2007) Proteomic analysis of metacyclic trypomastigotes undergoing *Trypanosoma cruzi*
 936 metacyclogenesis. *J Mass Spectrom* **42**: 1422-1432.
- 937 Pearl, L.H., and Prodromou, C. (2000) Structure and *in vivo* function of Hsp90. *Curr Opin*
 938 *Struct Biol* **10**: 46–51.
- 939 Pearl, L.H., and Prodromou, C. (2006) Structure and mechanism of the Hsp90 molecular
 940 chaperone machinery. *Annu Rev Biochem* **75**: 271–294.
- 941 Pollock, J.D., Williams, D.A., Gifford, M.A., Li, L.L., Du, X., Fisherman, J., *et al.* (1995)
 942 Mouse model of X-linked chronic granulomatous disease, an inherited defect in phagocyte
 943 superoxide production. *Nat Genet* **9**: 202-209.

- 944 Pratt, W.B., and Toft, D.O. (1997) Steroid receptor interactions with heat shock protein and
945 immunophilin chaperones. *Endocr Rev* **18**: 306–360.
- 946 Pratt, W.B., and Dittmar, K.D. (1998) Studies with purified chaperones advance the
947 understanding of the mechanism of glucocorticoid receptor-hsp90 heterocomplex assembly.
948 *Trends Endocrinol Metab* **9**: 244–252.
- 949 Pratt, W.B., Galigniana, M.D., Harrell, J.M. and DeFranco, D.B. (2004) Role of hsp90 and the
950 hsp90-binding immunophilins in signalling protein movement. *Cell Signal* **16**: 857-872.
- 951 Ratajczak, T., Ward, B.K., and Minchin, R.F. (2003) Immunophilin chaperones in steroid
952 receptor signalling. *Curr Top Med Chem* **3**: 1348–1357.
- 953 Ratajczak, T., Ward, B.K., Cluning, C. and Allan, R.K. (2009) Cyclophilin 40: An Hsp90-
954 cochaperone associated with apo-steroid receptors. *Int J Biochem Cell Biol* **41**: 1652-1655.
- 955 Riggs, D.L., Cox, M.B., Cheung-Flynn, J., Prapapanich, V., Carrigan, P.E., and Smith, D.F.
956 (2004) Functional specificity of co-chaperone interactions with Hsp90 client proteins. *Crit*
957 *Rev Biochem Mol Biol* **39**: 279–295.
- 958 Rosenzweig, D., Smith, D., Opperdoes, F., Stern, S., Olafson, R.W. and Zilberstein, D. (2008)
959 Retooling *Leishmania* metabolism: from sand fly gut to human macrophage. *FASEB J* **22**:
960 590-602.
- 961 Sacks, D.L. and Perkins, P.V. (1984) Identification of an infective stage of *Leishmania*
962 promastigotes. *Science* **223**: 1417-1419.
- 963 Seebach, T., Hemphill, A., and Lawson, D. (1990) The cytoskeleton of trypanosomes.
964 *Parasitol Today* **6**: 49–52.
- 965 Serafim, T.D., Figueiredo, A.B., Costa, P.A.C., Marques-da-Silva, E.A., Gonçalves, R., de
966 Moura, S.A.L., Gontijo, N.F., da Silva, S.M. et al. (2012) *Leishmania* metacyclogenesis is
967 promoted in the absence of purines. *PLoS Negl Trop Dis* **6**: e1833.

- 968 Silverman, J.M., Chan, S.K., Robinson, D.P., Dwyer, D.M., Nandan, D., Foster, L.J., and
969 Reiner, N.E. (2008) Proteomic analysis of the secretome of *Leishmania donovani*. *Genome*
970 *Biol* **9**: R35.
- 971 Silverman, J.M., Clos, J., Horakova, E., Wang, A.Y., Wiesgigl, M., Kelly, I., Lynn, M.A.,
972 McMaster, W.R., Foster, L.J., Levings, M.K., et al. (2010) *Leishmania* exosomes modulate
973 innate and adaptive immune responses through effects on monocytes and dendritic cells. *J*
974 *Immunol* **185**: 5011–5022.
- 975 Silverstein, A.M., Galigniana, M.D., Kanelakis, K.C., Radanyi, C., Renoir, J.M., and Pratt,
976 W.B. (1999) Different regions of the immunophilin FKBP52 determine its association with
977 the glucocorticoid receptor, hsp90, and cytoplasmic dynein. *J Biol Chem* **274**: 36980–36986.
- 978 Smith, M.R., Willmann, M.R., Wu, G., Berardini, T.Z., Möller, B., Weijers, D. and Poethig,
979 R.S. (2009) Cyclophilin 40 is required for microRNA activity in Arabidopsis. *Proc Natl*
980 *Acad Sci U S A* **106**: 5424-5429.
- 981 Spath, G.F., Epstein, L., Leader, B., Singer, S.M., Avila, H.A., Turco, S.J. and Beverley, S.M.
982 (2000) Lipophosphoglycan is a virulence factor distinct from related glycoconjugates in the
983 protozoan parasite *Leishmania major*. *Proc Natl Acad Sci U S A* **97**: 9258-9263.
- 984 Tolson, D.L., Schnur, L.F., Jardim, A. and Pearson, T.W. (1994) Distribution of
985 lipophosphoglycan-associated epitopes in different *Leishmania* species and in African
986 trypanosomes. *Parasitol Res* **8**: 537-542.
- 987 Uezato, H., Kato, H., Kayo, S., Hagiwara, K., Bhutto, A., Katakura, K., Nonaka, S., and
988 Hashiguchi, Y. (2005) The attachment and entry of *Leishmania (Leishmania) major* into
989 macrophages: observation by scanning electron microscope. *J Dermatol* **32**: 534–540.
- 990 Walczak, C.E. (2000) Microtubule dynamics and tubulin interacting proteins. *Curr Opin Cell*
991 *Biol* **12**: 52–56.

- 992 Walters, L.L., Modi, G.B., Chaplin, G.L., and Tesh, R.B. (1989) Ultrastructural development of
993 *Leishmania chagasi* in its vector, *Lutzomyia longipalpis* (Diptera: Psychodidae). *Am J Trop*
994 *Med Hyg* **41**: 295–317.
- 995 Walters, L.L., Irons, K.P., Chaplin, G., and Tesh, R.B. (1993) Life cycle of *Leishmania major*
996 (Kinetoplastida: Trypanosomatidae) in the neotropical sand fly *Lutzomyia longipalpis*
997 (Diptera: Psychodidae). *J Med Entomol* **30**: 699–718.
- 998 Ward, B.K., Allan, R.K., Mok, D., Temple, S.E., Taylor, P., Dornan, J et al. (2002) A structure-
999 based mutational analysis of cyclophilin 40 identifies key residues in the core
1000 tetratricopeptide repeat domain that mediate binding to Hsp90. *J Biol Chem* **277**: 40799–
1001 40809.
- 1002 Warth, R., Briand, P.A. and Picard, D. (1997) Functional analysis of the yeast 40 kDa
1003 cyclophilin Cyp40 and its role for viability and steroid receptor regulation. *Biol Chem* **378**:
1004 381-391.
- 1005 Weisman, R., Creanor, J. and Fantes, P. (1996) A multicopy suppressor of a cell cycle defect in
1006 *S. pombe* encodes a heat shock inducible 40 kDa cyclophilin-like protein. *EMBO J* **15**: 447-
1007 456.
- 1008 Wiesgigl, M. and Clos, J. (2001) Heat Shock Protein 90 Homeostasis Controls Stage
1009 Differentiation in *Leishmania donovani*. *Mol Biol Cell* **12**: 3307-3316.
- 1010 Yau, W.L., Blisnick, T., Taly, J.F., Helmer-Citterich, M., Schiene-Fischer, C., Leclercq, O., et
1011 al. (2010) Cyclosporin A treatment of *Leishmania donovani* reveals stage-specific functions
1012 of cyclophilins in parasite proliferation and viability. *PLoS Negl Trop Dis* **4**: e729.
- 1013 Zakai, H.A., Chance, M.L. and Bates, P.A. (1998) *In vitro* stimulation of metacyclogenesis in
1014 *Leishmania braziliensis*, *L. donovani*, *L. major* and *L. mexicana*. *Parasitology* **116**: 305-309.

1015 Zhang, W.W., Charest, H., Ghedin, E. and Matlashewski, G. (1996) Identification and
1016 overexpression of the A2 amastigote-specific protein in *Leishmania donovani*. *Mol Biochem*
1017 *Parasitol* **78**: 79-90.

1018 Zilberstein, D. and Shapira, M. (1994) The role of pH and temperature in the development of
1019 *Leishmania* parasites. *Annu Rev Microbiol* **48**: 449-470.

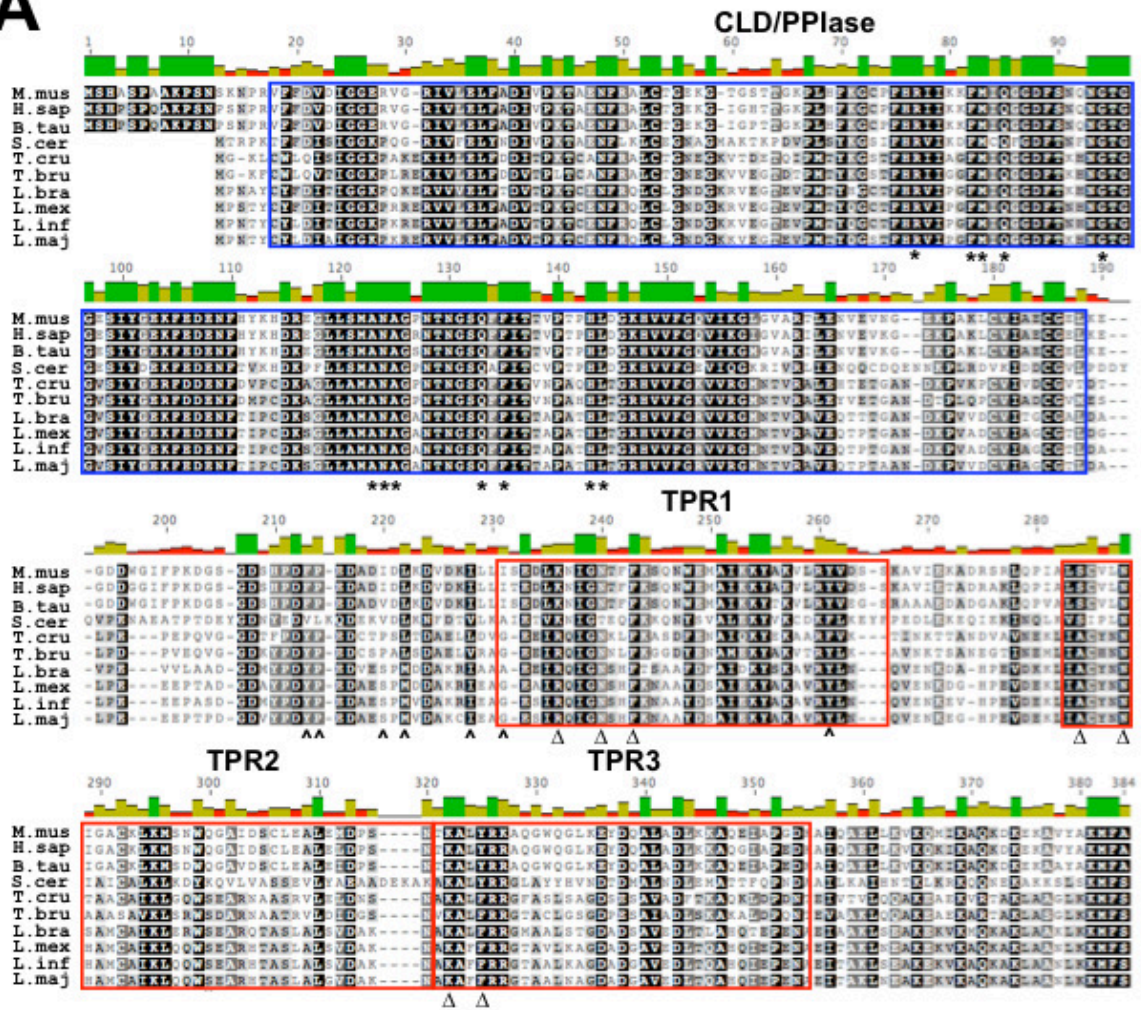
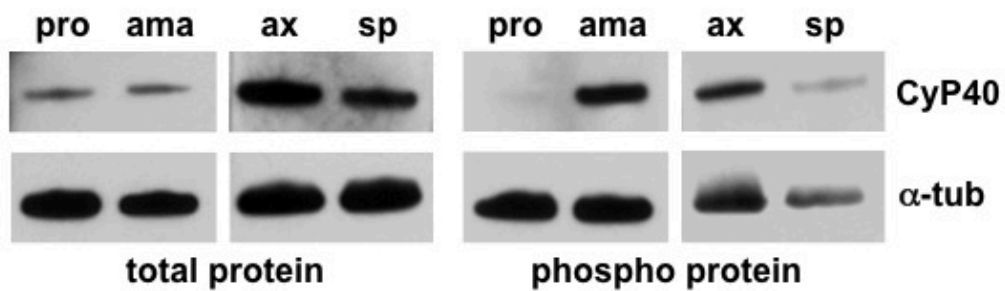
1020

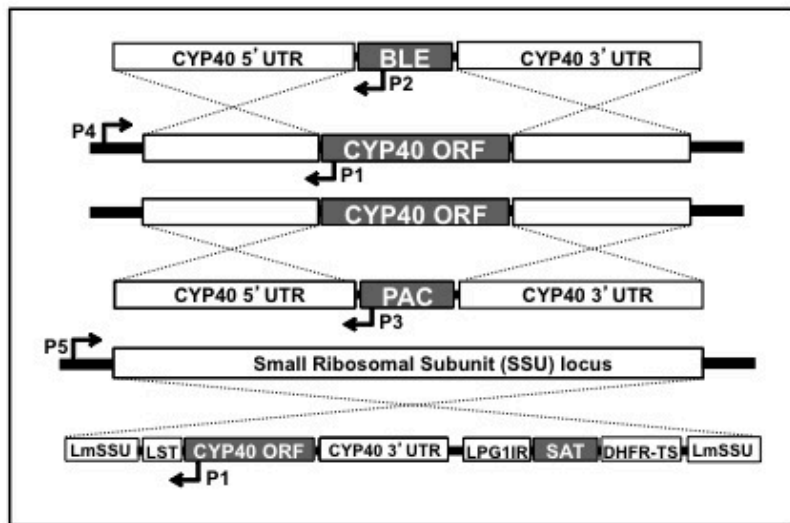
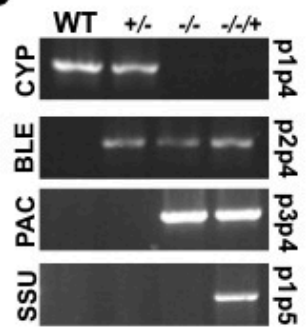
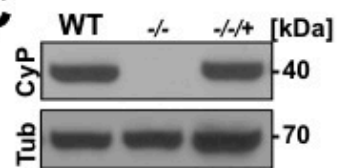
1021

1022

1023

1024

A**B****Figure 1**

A**B****C****Figure 2**

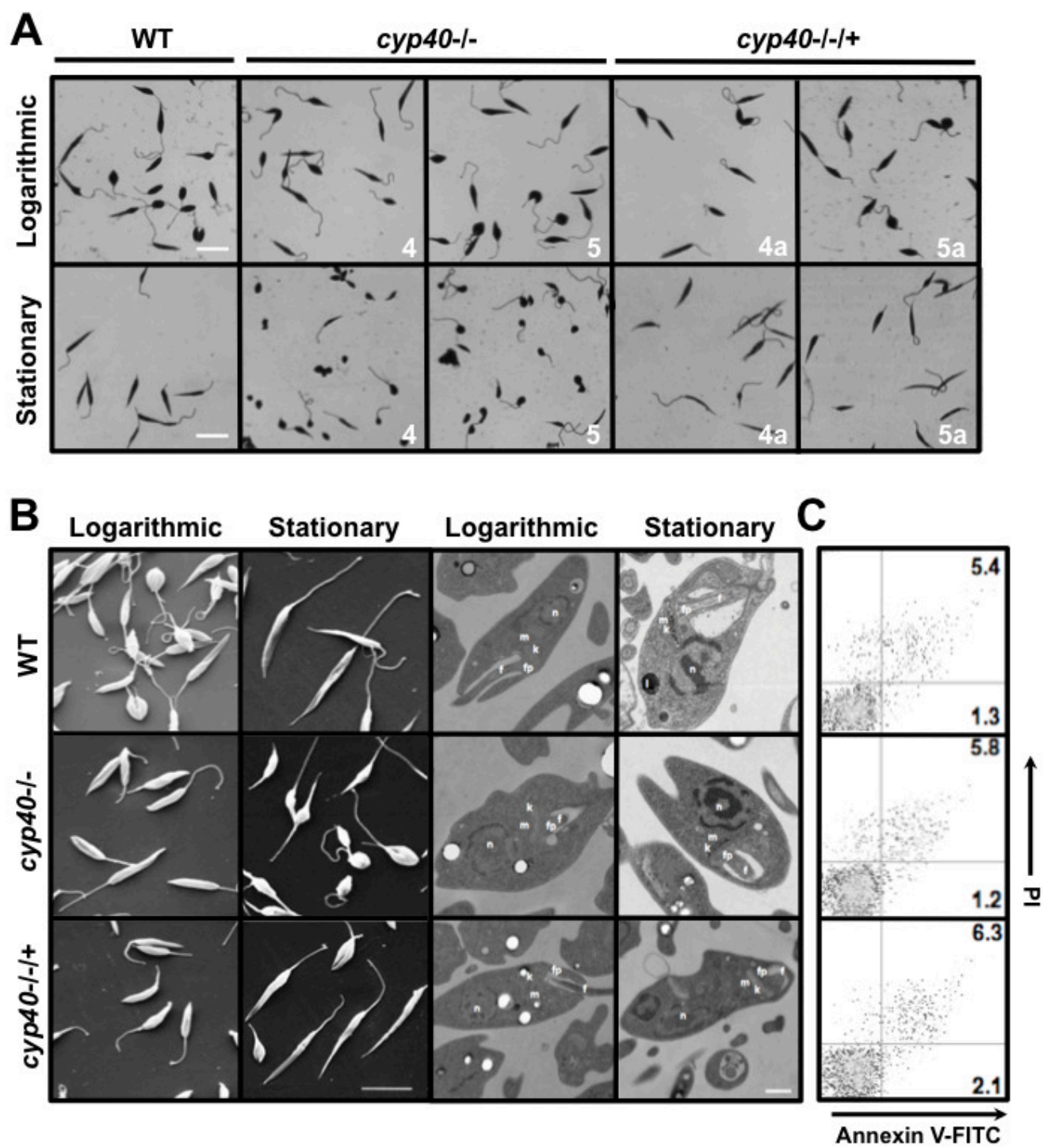


Figure 3

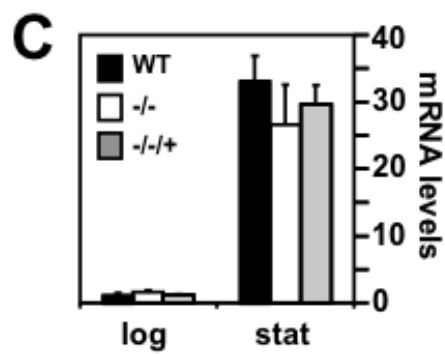
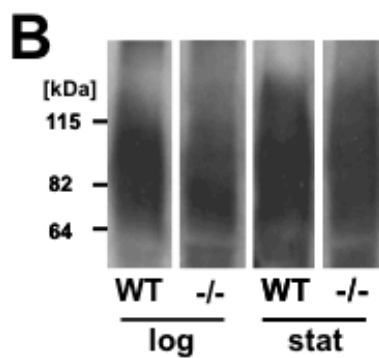
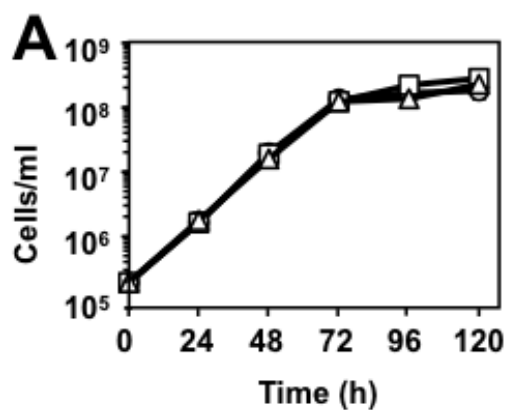


Figure 4

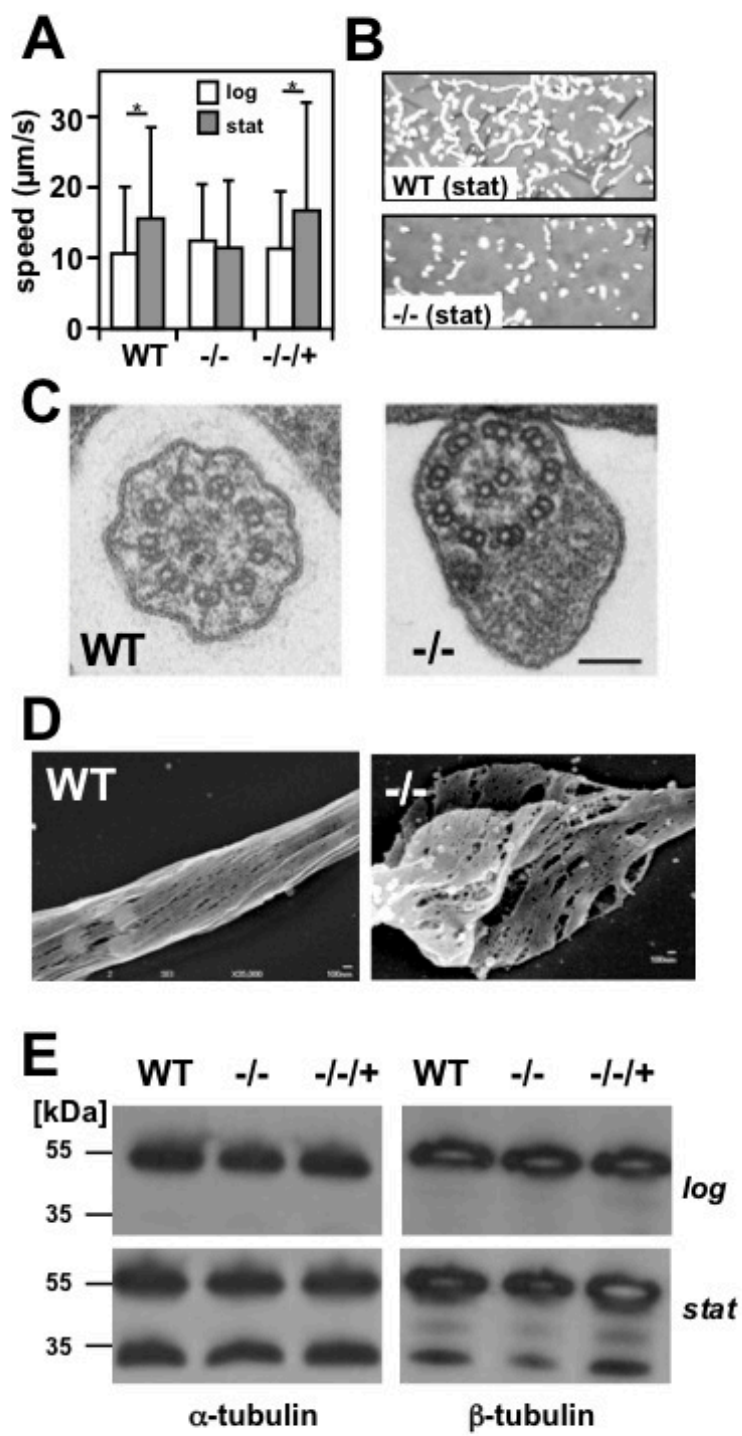


Figure 5

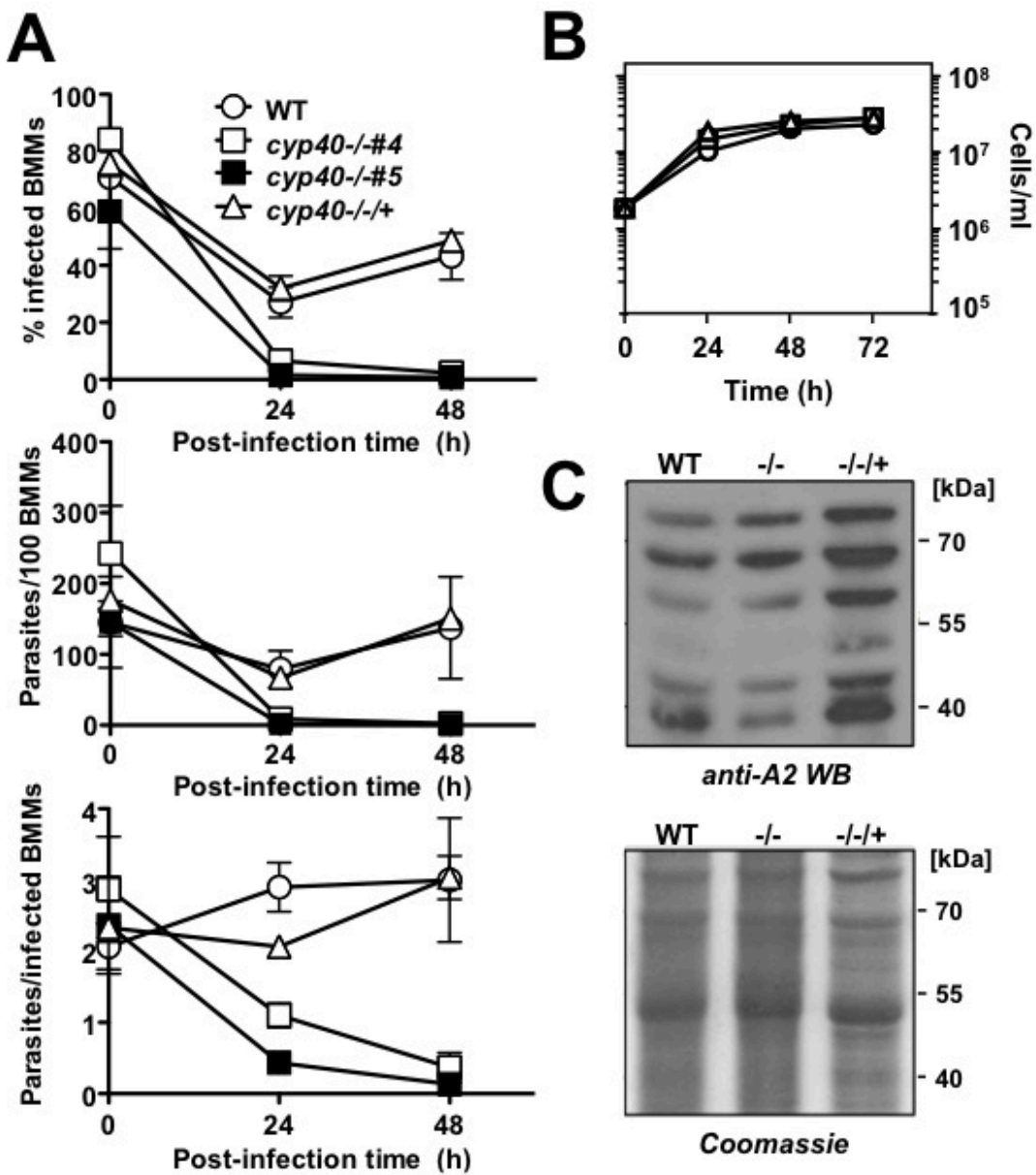


Figure 6

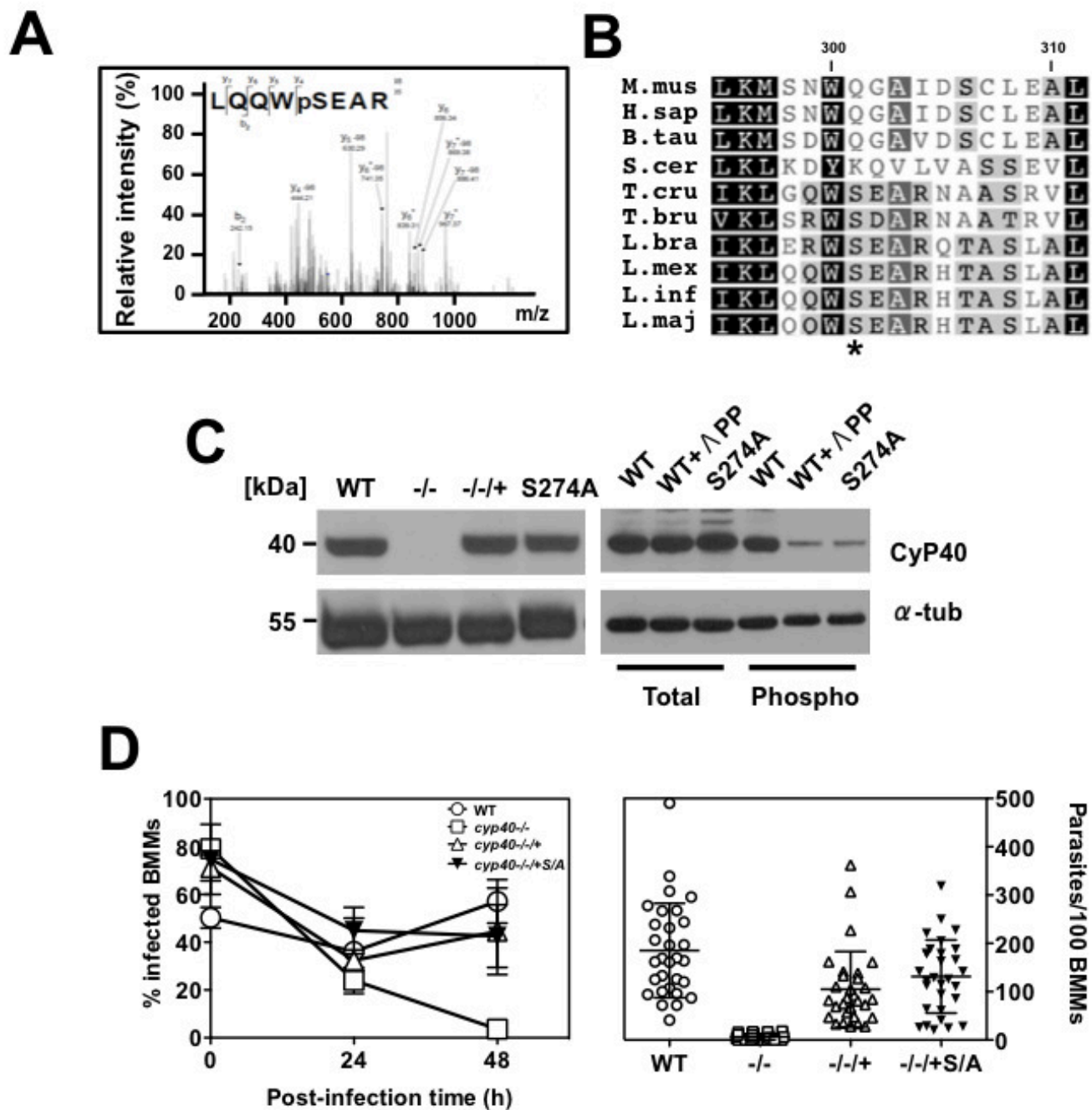


Figure 7

LinJ.35.4830

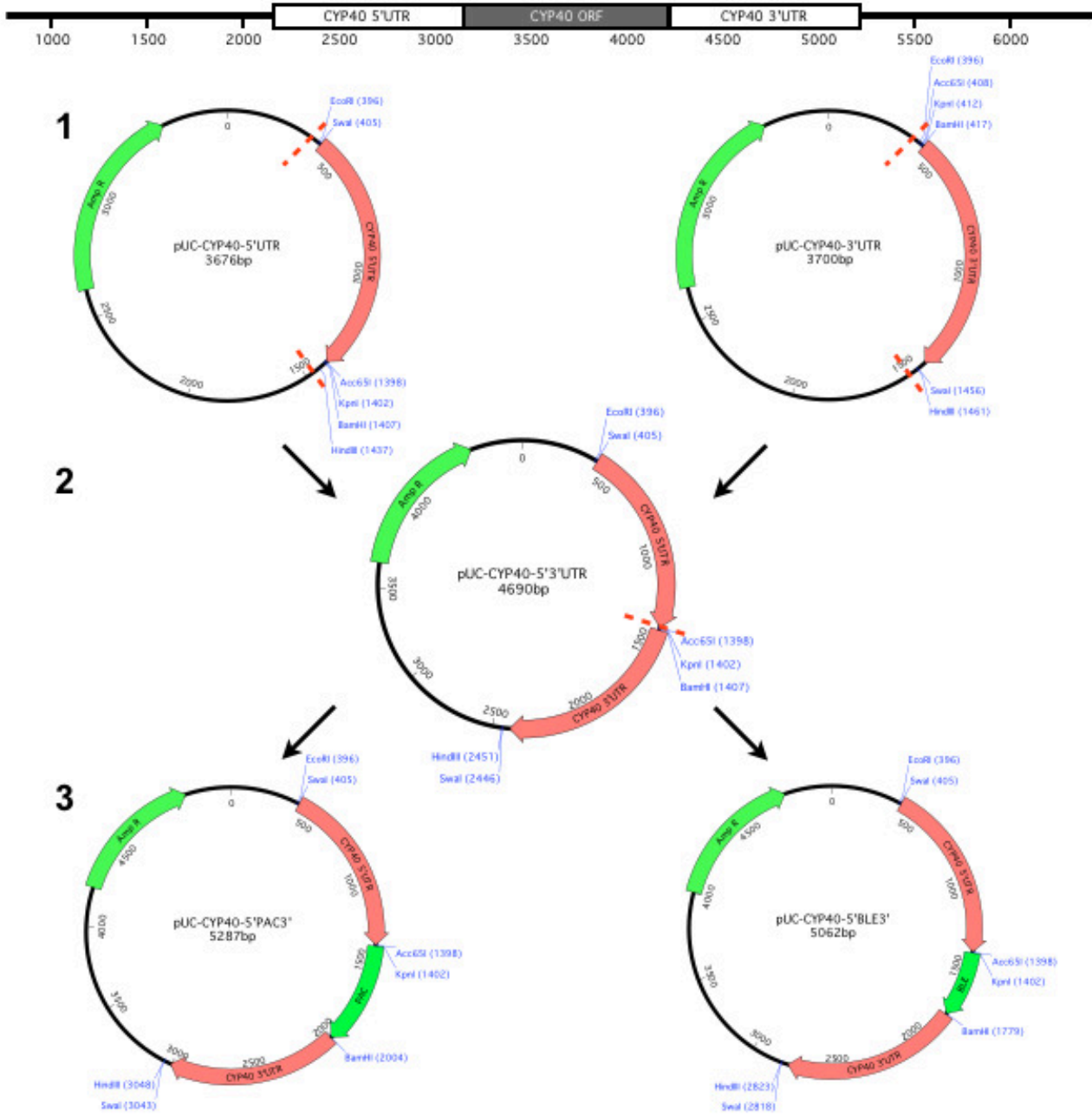


Figure S1

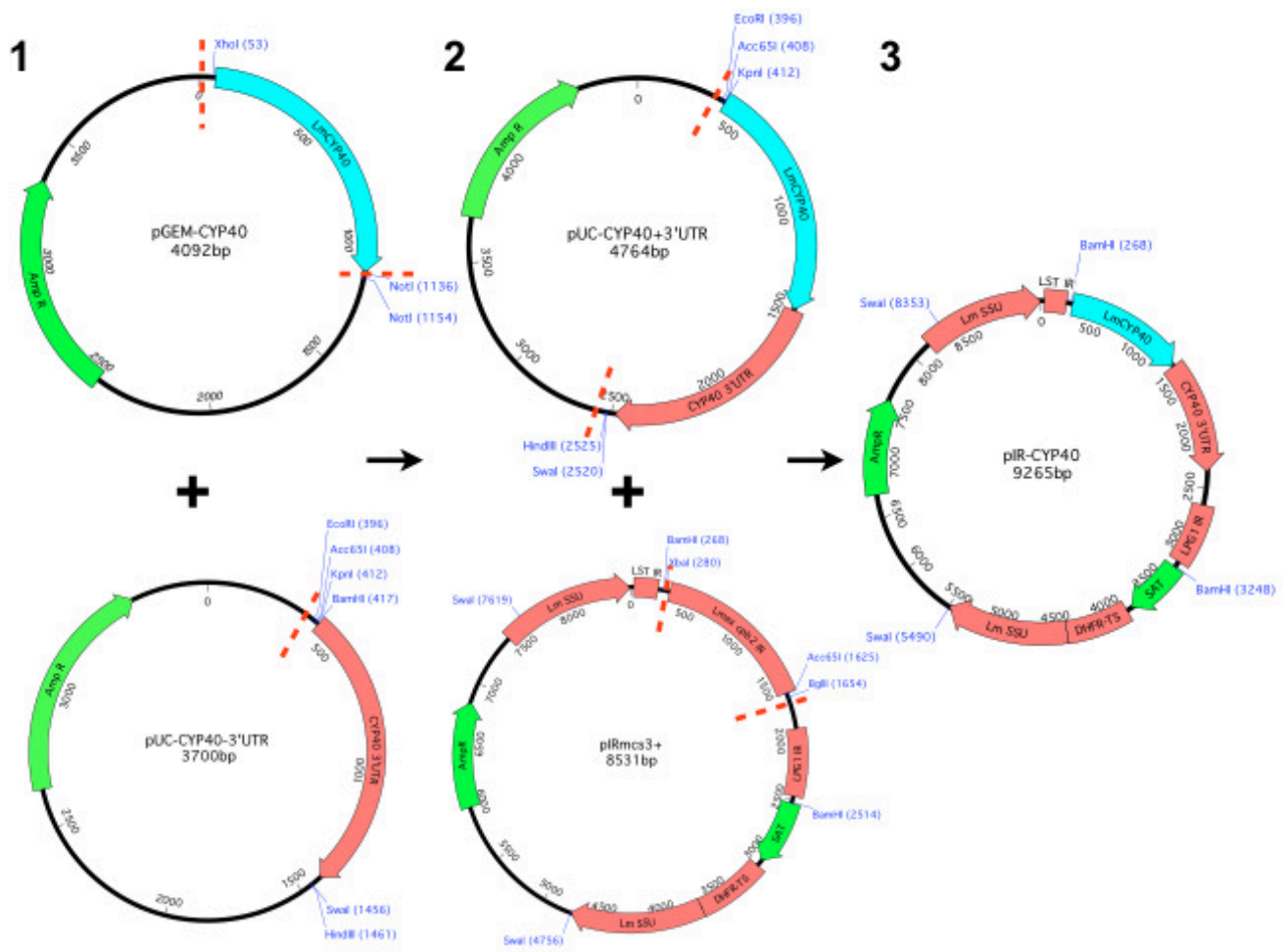


Figure S2

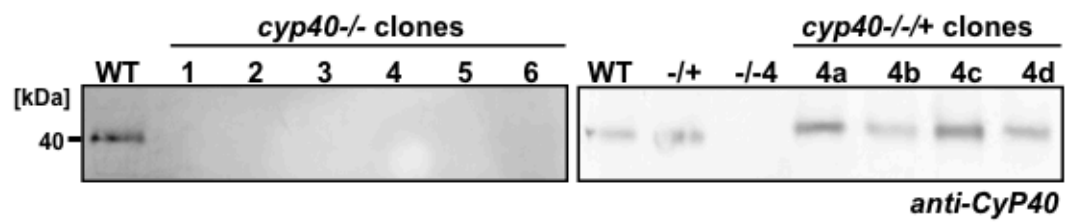


Figure S3

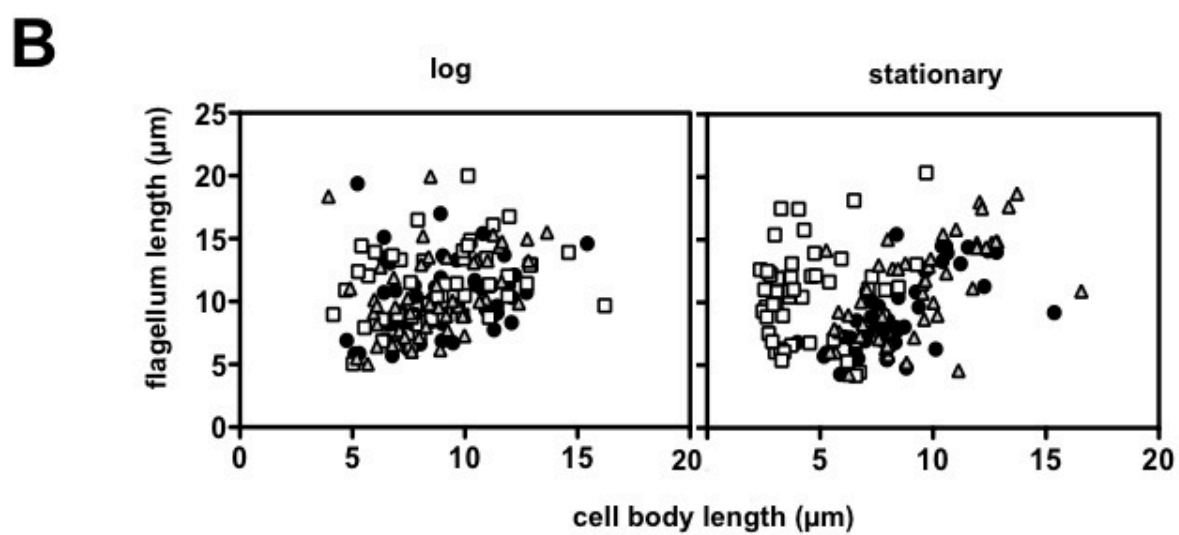
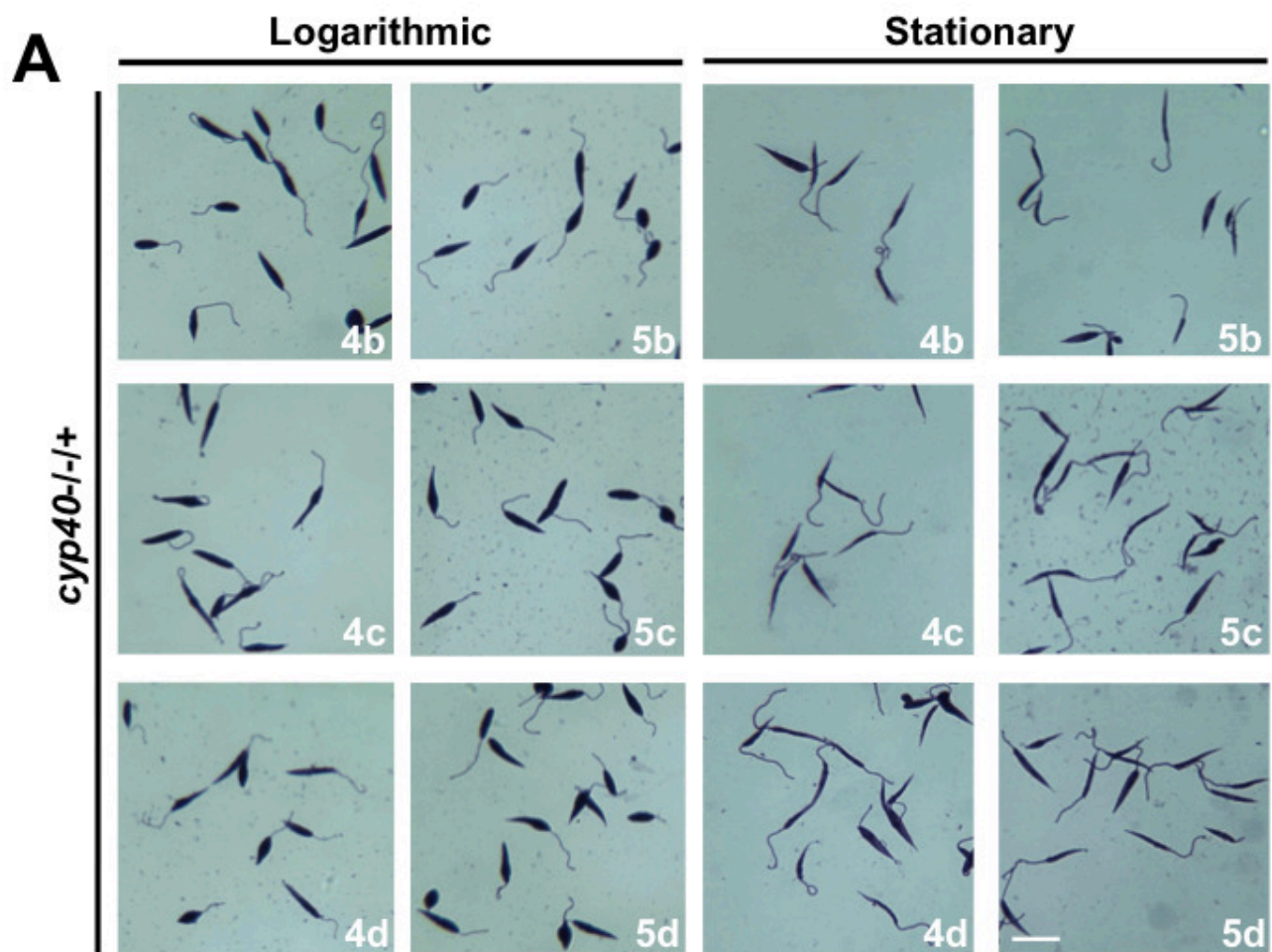
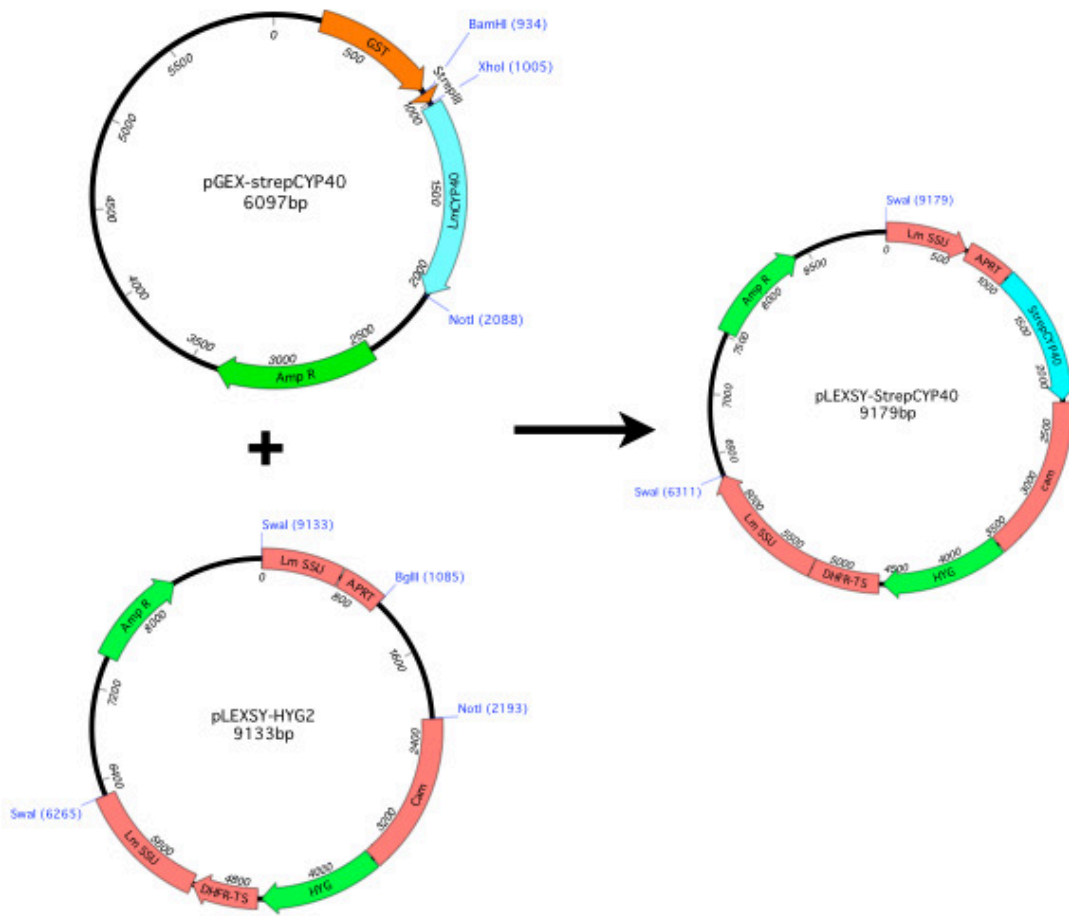
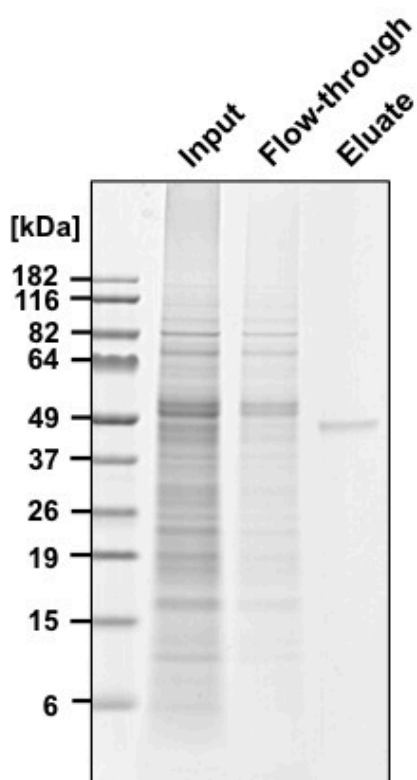
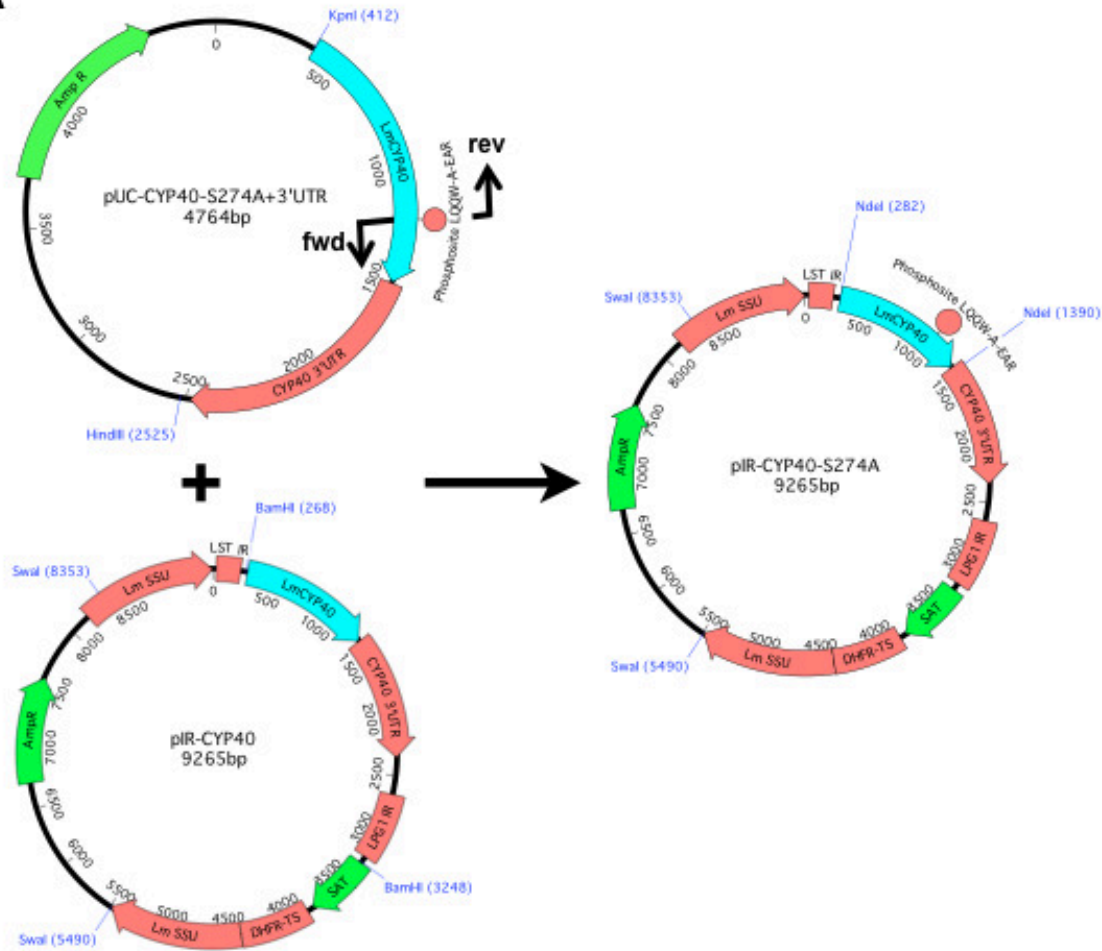
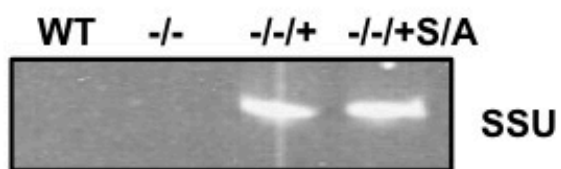


Figure S4

A**B****Figure S5**

A**B****Figure S6**

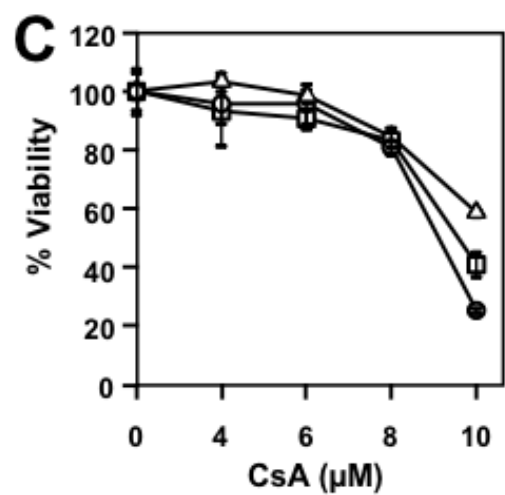
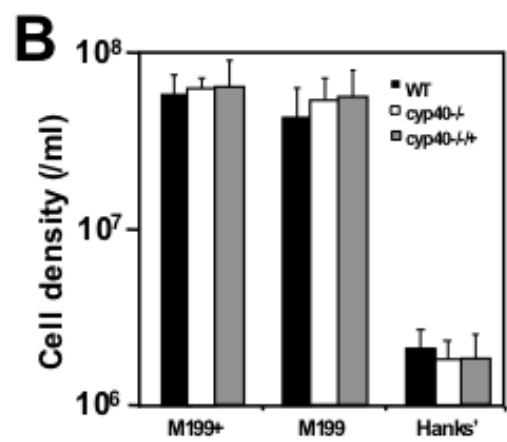
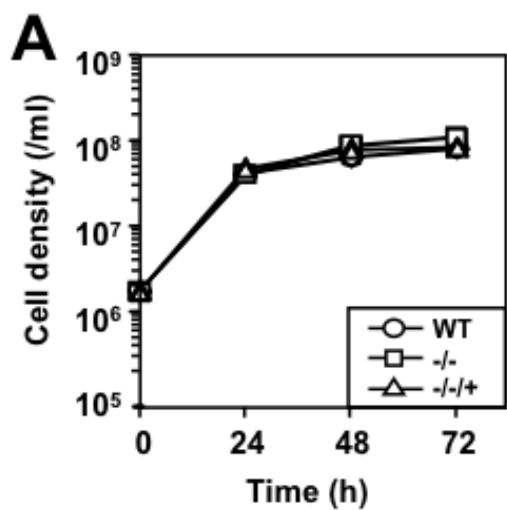


Figure S7